

# Measuring price impact and information content of trades in a time-varying setting

Francesco Campigli\*    Giacomo Bormetti†    Fabrizio Lillo‡§¶

## Abstract

We propose a non-linear observation-driven version of the Hasbrouck (1991) model for dynamically estimating trades' market impact and information content. We find that market impact displays an intraday pattern superimposed with large fluctuations. Some of them are exogenous, and, as an example, we investigate market impact dynamics around FOMC announcements. Contrary to Hasbrouck (1991), we find that the information content of trades depends on the local liquidity level and the recent history of prices and trades. Finally, we use the model to estimate the time-varying permanent impact parameter, which allows performing a dynamic transaction cost analysis.

---

\*Scuola Normale Superiore, Pisa, Italy. Email address: francesco.campigli@sns.it

†Dipartimento di Matematica, Università di Bologna, Bologna, Italy. Email address: giacomobormetti@unibo.it

‡Dipartimento di Matematica, Università di Bologna, and Scuola Normale Superiore, Pisa, Italy. Email address: fabrizio.lillo@unibo.it

§The authors thank the participants of the Sofie 2023 Conference (Seoul) and of the International Association for Applied Econometrics Conference - IAAE 2023 (Oslo) for useful comments and suggestions. GB and FL acknowledge financial support from the Italian Ministry MUR under the PRIN project *Dynamic models for a fast-changing world: An observation driven approach to time-varying parameters* (grant agreement no. 20205J2WZ4).

¶The authors thank Dr. German Rodikov, Dipartimento di Matematica, Università di Bologna german.rodikov@unibo.it for the important support to this work.

**Keywords:** Price impact; Information Content of Trades; Transaction Cost Analysis; Dynamic Conditional Score-driven Models.

**JEL classification:** C32; C51; C58; G14 .

## 1 Introduction

One of the most important challenges in market microstructure is the modeling and empirical estimation of how information is impounded into prices (O’Hara (2003)). Financial markets are characterized by an asymmetry between informed traders and uninformed liquidity providers. A series of seminal stylized models, starting from those of Glosten and Milgrom (1985) and Kyle (1985), clarified that traders’ information is slowly incorporated into prices through trading, which progressively reveals information to the market and leads to changes in prices and in the order flow. Thus, the price discovery process depends on how prices react to trades, an important quantity termed *price impact*, and on the market’s reaction to the past price and trade dynamics. At least two types of price impact emerge from this stylized description: the *instantaneous impact*, which describes the immediate price change caused by trade, and the *long term impact*, which describes the long-term price change taking into account the subsequent order flows and price changes triggered by the trade. Hasbrouck (1991a) identified the long-term impact as a measure of the information content of trade.

Understanding and modeling price impact is also of paramount importance in several financial applications. Market impact is the main source of transaction cost for large investors and optimal execution schemes (Almgren and Chriss (2001)), aiming at minimizing impact costs depending crucially both on the impact model and on the reliability of the estimated model parameters. From an empirical perspective, understanding the price discovery process is tantamount to modeling the joint dynamics of price changes and trades (or, more generally, orders). In the early Nineties, the pioneering work of Hasbrouck (1991a) paved the way for a modeling framework of the relationships between trades and quotes by proposing

a Structural Vector Auto-Regressive (SVAR) model of price changes and trade signs<sup>1</sup> for studying how prices incorporate information. In the model, the instantaneous impact of the market is described by a parameter that gives the proportionality factor between the sign of the trade at a certain time and the contemporaneous price change; the long-term impact, and thus the information content of a trade, is estimated as the cumulative long-term impulse response function of the SVAR. It is important to notice, also to better understand our contribution below, that Hasbrouck’s model is linear and with constant parameters, thus impacts and information content are constant and do not depend on time or on market conditions. Hasbrouck’s findings show that trades convey substantial information (Hasbrouck (1988)) that causes a persistent impact on prices (Hasbrouck (1991b)). Analysis shows that long-term impact arrives only with long delays and varies between securities (Hasbrouck (1991a)). Hautsch and Huang (2012) show that limit orders also have a long-term effect on prices, while Dufour and Nguyen (2012) document the long-term impact of trade on the bond market. Extending the VAR models, Engle and Patton (2004) proposed a non-linear VAR to describe the possible role of volume in the information content of the trade, and Barclay et al. (2003) developed a multiple equation VAR system, which includes a trade indicator variable for each of the market participants.

More recently Philip (2020) proposed a Reinforcement Learning framework to reinterpret an extended version of the original Hasbrouck’s model. Although groundbreaking, subsequent research has highlighted some important limitations of Hasbrouck’s SVAR approach. Dufour and Engle (2000) generalized the original VAR model by introducing a temporal dummy variable, measuring the effect of the time of the trade on the permanent impact. They argued that the price impact and liquidity depend on the frequency of the trading activity, which varies over the day. In this regard, the work challenges the assumption of constant liquidity. Using a different setting, Cont et al. (2014) and Mertens et al. (2021) find that price changes are mainly driven by liquidity, which exhibits significant intraday variations, challenging the

---

<sup>1</sup>It is widely accepted that trade size has a small incremental explanatory power beyond trade sign when estimating the SVAR model (see Hasbrouck (2007)).

constant impact assumption. Philip (2020) shows that SVAR models are misspecified and can produce incorrect inferences when the price impact function is non-linear.

In this paper, we propose an extension of Hasbrouck’s framework which fixes several of the above limitations, postulating a non-linear relation between trade signs and price changes. Specifically, our framework considers the probability of a certain type of trade, uses a clever aggregation and parameterization scheme to consider hundreds of lags, and models a time-varying instantaneous market impact that adapts itself to recent price and trade history. The time-varying setting is based on the Dynamic Conditional Score-Driven Approach (DCS) of Creal et al. (2013) and Harvey (2013). Among the observation-driven models, DCS provides a general framework for time-varying parameter models. The key ingredient in DCS models is that the scaled score updates the time-varying parameters. This update rule cleverly exploits the observation density and includes many existing models <sup>2</sup>. Due to ease of estimation, high flexibility, and wide application range, DCS models represent a valuable alternative to other observation- and parameter-driven models. Moreover, as it will be clear for our models, the DCS approach can be seen as a filter of misspecified dynamics of the time-varying parameters.

The present work brings different contributions to the literature, developing a modified score-driven version of the SVAR model by Hasbrouck (1991a). First, we do not model the evolution of the trade sign process directly but we focus on the evolution of the occurrence probability of a buy trade. We employ an inverse logistic function to describe the dynamics of the trading indicator, consistent with its binary nature. Our specification provides a better-specified description of the trade-sign time series, as confirmed by several tests run on the model’s residuals. Second, we aggregated lagged values of the order flow variable of the modified model on three different scales following the technique introduced in Corsi (2009) to mimic the persistence of the realized volatility. The aggregation allows us to mitigate the curse of dimensionality while capturing the well-known persistence of the order flow (see Lillo and Farmer (2004); Toth et al. (2015)), while at the same time improving

---

<sup>2</sup>For instance, see Normal GARCH by Bollerslev (1986), ACD by Engle and Russell (1998), and MEM by Engle and Gallo (2006).

the quality of the model specification. As the last and most significant modification in our model, the instantaneous impact parameter of trades on quotes and the volatility of the return idiosyncratic component are time-varying and follow score-driven integrated dynamics. We derive the score-driven aggregated modified Hasbrouck model (SDAMH) equations by computing the log-likelihood function and the scaled score needed for the DCS updating of the instantaneous impact and volatility.

We empirically test our approach by estimating the SDAMH model on a sample of data of Apple Inc. (AAPL), Microsoft (MSFT), Alphabet Inc. (GOOG) and Amazon (AMZN) stocks listed on NASDAQ. We take into consideration these stocks, as they show different microstructural properties: AAPL and MSFT can be considered large-tick stocks, while AMZN and GOOG are small-tick stocks. Our choice allows to analyze the effect of tick size on the price impact and on the information content of stock trades. Since the results for stocks with similar tick sizes are homogeneous, we report estimates only for MSFT and AMZN, while the others are available upon request. Estimates show that integrated DCS dynamics reproduce the relevant features of the volatility and the instantaneous impact. Concerning the latter, we find that it displays an intraday decreasing pattern, being large at the beginning of the day and declining afterward, and displaying some large localized fluctuations, possibly related to endogenously or exogenously driven liquidity crises. As a specific case of the latter, we study in detail the days of the Federal Open Market Committee (FOMC) announcements. To estimate the time-varying information content of trades, we estimate the long-run value of the Cumulative Impulse Response Function (CIRF) computed using Monte Carlo simulation. The analysis reveals that the information content of the stock trades varies mainly according to two factors: The instantaneous impact parameter and the *state* of the market in a specific trade. The *state* corresponds to the conditional mean of the SDAMH model, ignoring the impact of the last trade. We further unravel these findings using linear regressions, which confirm that the permanent impact positively depends on the instantaneous time-varying impact and negatively on the conditional mean of the model. These findings are in clear

contrast to the Hasbrouck (1991a) SVAR model, where the information content is constant and independent of the state of the market. Analysis of the CIRF dynamics around FOMC announcements confirms the ability of the impact parameter in the DCS specification to react quickly to changing market conditions.

Last but not least, we advocate the relevance of our approach in transaction cost analysis. This task requires a careful estimation of the permanent impact of trade since the implementation shortfall depends crucially on this parameter. Standard practice for its estimation (see, for example, Cartea and Jaimungal (2016)) regresses the price increments aggregated over a macroscopic time scale (typically 5 minutes) on aggregated transaction volumes across a long period (typically one day). This leads to a static estimation, which does not use all available data and does not dynamically adapt to changing market conditions. At variance, we exploit the complete information content of tick-by-tick price and trade time series and derive the (approximate) analytic permanent impact function of the SDAMH model. Our formula quantifies the effect of a single transaction on mid-quote returns using the model's estimated coefficients. However, the SDAMH model avoids data aggregation and takes advantage of the information content of the time series of the price and the trade more efficiently, thus providing a lower standard error. We tested the two approaches on the MSFT and AMZN stocks. The permanent impact coefficient estimated using SDAMH is more accurate than the one obtained with Cartea and Jaimungal (2016). This fact opens the possibility of running a dynamical transaction cost analysis and performing optimal execution conditionally on the intraday time.

The rest of the paper is organized as follows. In section 2, we derive the equations of the SDAMH model and describe the estimation procedure of the model's parameters. Section 3 presents an empirical application of the SDAMH model to actual data. We report the ML estimates of the model's static parameters and plot the filtered time-varying impact and of the volatility over the entire sample. We investigate the implications of a time-varying impact and market *state* on the conditional information content of stock trades. In Section 4,

we focus on the behavior of the permanent impulse in the case of the FOMC announcement of June 16, 2021. In section 5, we show the relevance of our approach for transaction cost analysis and optimal execution, deriving the approximate permanent impact expression from the model parameters and comparing it with the alternative method discussed in Cartea and Jaimungal (2016). Section 6 concludes.

## 2 The SDAMH model

To study the joint dynamics of trades and prices and to measure the information content of a trade, Hasbrouck (1991a) proposed the following model

$$\begin{aligned} r_t &= \sum_{i=1}^p a_i r_{t-i} + \sum_{i=0}^p b_i x_{t-i} + v_{1,t}, \\ x_t &= \sum_{i=1}^p c_i r_{t-i} + \sum_{i=1}^p d_i x_{t-i} + v_{2,t}, \end{aligned} \tag{1}$$

where  $t \in \mathbb{N}$  is the trade time,  $r_t = (q_t - q_{t-1})/q_{t-1}$  is the mid-point price return<sup>3</sup>,  $q_t$  being the mid-point just after the trade at time  $t$ , and  $x_t \in \{-1, +1\}$  is a trading dummy indicator for sell/buy orders of the trade at time  $t$ . The noise terms  $v_{1,t}$  and  $v_{2,t}$  have variances  $\sigma_1^2$  and  $\sigma_2^2$ , respectively, and  $\rho$  is their correlation, which is set to zero to make the model identifiable. Eq. (1) describes a SVAR model where  $b_0$ , the structural parameter, describes the contemporaneous effect between  $r_t$  and  $x_t$ . From a financial point of view,  $b_0$  describes the instantaneous impact of a trade. SVAR model parameters can be estimated using ordinary least square (OLS) and their analytical tractability allows to derive the impulse response function (IRF) expressed as a function of the estimated parameters in closed form solution (see Lütkepohl (2005)). Moreover, following the interpretation of Hasbrouck, the asymptotic cumulative IRF measures the long-term effect of trade on prices and thus represents the

---

<sup>3</sup>Other choices are possible. The original Hasbrouck (1991a) paper uses the mid-quote price change, while Philip (2020) uses the change in the natural logarithm of the mid-point. On these very short timescales, the different definitions lead to negligible differences.

information content of trade. Hasbrouck’s model assumes that the information content of a trade is constant in the investigated period. This is a consequence of the fact that the parameters in Eq. (1) are constant and of the linear structure of the model. Indeed, it is well known that for a VAR model, the IRF does not depend on the history of the process, but only on the parameters of the model (Lütkepohl (2005)). However, the information content of trade is unlikely to be constant throughout the day, and one can expect that the arrival of news, for example, an FOMC meeting, or the hectic intraday dynamics can dramatically modify it. Furthermore, the fluctuating nature of liquidity makes the response of price to trade not constant, which cannot be captured by Eq. (1). In this paper, we propose a model for measuring the *dynamics* of liquidity and of the information content of a trade by proposing a time-varying parameter version of Hasbrouck’s model. To this end, we rely on the DCS approach of Creal et al. (2013) and Harvey (2013). To introduce it, consider a sequence of observations  $\{z_t\}_{t=1}^T$ , where each  $z_t \in \mathbb{R}^M$ , and a conditional probability density  $P(z_t|f_t)$ , that depends on a vector of time-varying parameters  $f_t \in \mathbb{R}^W$ . Defining the score as  $\nabla_t := \partial \log P(z_t|f_t)/\partial f_t'$ , a score-driven model assumes that the dynamics of the parameters follows

$$f_{t+1} = \omega + \beta f_t + \alpha s_t \quad \text{where} \quad s_t := (\mathcal{I}_{t|t-1})^{-1} \nabla_t \quad (2)$$

and  $\mathcal{I}_{t|t-1}$  is the Fisher information matrix. In Eq. (2)  $\omega$  is a vector of dimensions  $W$ ,  $\alpha$  and  $\beta$  are matrices  $W \times W$  of static parameters. Interestingly, one can consider a score-driven model as either a data-generating process (DGP) or a filter of unknown dynamics. In both cases, the most important feature of Eq. (2) is the role of the score as the driver of the dynamics of  $f_t$ . The dependence of  $f_{t+1}$  on the vector of observations  $z_t$  follows from the conditional density specification, which determines the score. Thanks to the random occurrence of  $z_t$ , the updating rule provides stochastic dynamics when one looks at the model as a DGP. When regarded as a filter, the update rule in Eq. (2) delivers a sequence of filtered parameters  $\{\hat{f}_t\}_{t=1}^T$ . Maximizing the log-likelihood of the whole sequence of observations provides an estimate of the static parameters. Score-driven models have seen an explosion of



interest in recent years <sup>4</sup> due to their flexibility and ease of estimation. Many state-of-the-art popular econometric models belong to the family of score-driven models. Examples are the GARCH model, the Exponential GARCH model, the Autoregressive Conditional Duration model, and the Multiplicative Error Model. In this paper, we develop a DCS version of Hasbrouck’s model to describe and filter the time-varying dynamics of market impact, return volatility, and information content of a trade. To this end, we assume that the parameters  $b_0$  and  $\sigma_1^2$  of Eq. (1) are time-varying according to DCS dynamics. Our choice is minimal because one could build a model where all the parameters of Eq. (1) follow a DCS model. However, the complexity of the model would grow significantly and the estimation of the model would be computationally more difficult. We believe that  $b_0$  captures an important part of the relation between trades and prices, and for this reason, in this paper, we explore its dynamics. To build a DCS version of the Hasbrouck model it is necessary to specify the conditional probability density  $P(z_t|f_t)$  of the model. In the original formulation of Eq. (1) the distribution of the noise terms  $v_{1,t}$  and  $v_{2,t}$  is not specified <sup>5</sup>. Moreover, the binary nature of  $x_t$  requires a complicated temporal dependence structure for  $v_{2,t}$ . Therefore, we modify the original model to specify the probability density of the observables. In particular, we replace the second equation in Eq. (1) by using an inverse logistic map for  $\mathbb{P}(x_t = +1|\mathcal{F}_{t-1})$ , where  $\mathcal{F}_t$  is the available information set at time  $t$

$$r_t = \mu_1 + \sum_{i=1}^p a_i r_{t-i} + \sum_{i=0}^p b_i x_{t-i} + v_{1,t},$$

$$\mathbb{P}(x_t = +1|\mathcal{F}_{t-1}) := \pi_t = \text{Logit}^{-1}\left(\mu_2 + \sum_{i=1}^p c_i r_{t-i} + \sum_{i=1}^p d_i x_{t-i}\right), \quad (3)$$

where  $\text{Logit}^{-1}(z) = (1 + e^{-z})^{-1}$  is the inverse logistic map of  $z$  and we assume that  $v_{1,t} \sim \mathcal{N}(0, \sigma^2)$ . Notice that we have also added two constant parameters,  $\mu_1$  and  $\mu_2$ , to include possible drift effects on price returns and trade signs. The Modified Hasbrouck’s (MH) model

---

<sup>4</sup>See for example <http://www.gasmodel.com>.

<sup>5</sup>Remember that the estimation is performed via OLS.

of Eq. (3) explicitly provides the form of the conditional density, as required to build a DCS time-varying parameter version, and can be estimated by using the Maximum Likelihood Estimator (MLE). The transformation we use provides two main advantages. First, the inverse logistic transformation is consistent with the binary nature of the trading dummy indicator. Second, it introduces nonlinearity in the model. Philip (2020) demonstrates that when the permanent impact function has a linear relationship with the trade sign, the model is highly misspecified. The logistic transformation makes the relationship between the permanent impact function (we will see this later in detail) and the trade sign variable non-linear. As pointed out later, these modifications make the IRF non-linear and no longer available in a closed-form solution. Before presenting the DCS version of Hasbrouck’s model, we present a second modification of Eq. (1). The number of parameters to estimate in Hasbrouck’s model depends on the number of lags  $p$  in the VAR equations. The original Hasbrouck (1991a) uses  $p = 5$ , but several more recent papers found this number too small to reproduce the dynamics of trades and prices. For example, a vast body of literature found that the order flow process  $x_t$  is consistent with a long memory process Bouchaud et al. (2003); Lillo and Farmer (2004); Bouchaud et al. (2009); Toth et al. (2015); Bouchaud et al. (2018). To avoid the use of a large  $p$ , and thus the estimation of a large number of parameters, we employ the technique developed in Corsi (2009) for the time aggregation of regressors in realized volatility models and used in the market microstructure by Hasbrouck (2021). Let define  $L_1, L_2 \in \mathbb{N}$  two integers indicating the number of past lags we consider for the aggregation. Consequently, we introduce the aggregated variables  $x_t^{(L_1)} := \frac{1}{L_1-1} \sum_{i=2}^{L_1} x_{t-i}$  and  $x_t^{(L_2)} := \frac{1}{L_2-L_1} \sum_{j=L_1+1}^{L_2} x_{t-j}$  and use them as regressors of the VAR together with  $r_{t-1}$  and  $x_{t-1}$ <sup>6</sup>. In the following, we choose  $L_1 = 10$  and  $L_2 = 100$ . Then, the model reads

$$\begin{aligned} r_t &= \mu_1 + a_1 r_{t-1} + b_0 x_t + b_1 x_{t-1} + \bar{b}_{10} x_t^{(10)} + \bar{b}_{100} x_t^{(100)} + v_{1,t}, \\ \pi_t &= \text{Logit}^{-1} \left( \mu_2 + c_1 r_{t-1} + d_1 x_{t-1} + \bar{d}_{10} x_t^{(10)} + \bar{d}_{100} x_t^{(100)} \right), \end{aligned} \quad (4)$$

---

<sup>6</sup>It is not necessary to define aggregated regressors for the  $r_t$  process as the midpoint price returns do not show long memory property.

where  $\mu_1, \mu_2, a_1, b_0, b_1, \bar{b}_{10}, \bar{b}_{100}, c_1, d_1, \bar{d}_{10}, \bar{d}_{100}$  and  $\sigma^2$  are constant. We term this model the Aggregated Modified Hasbrouck (AMH) model. In the online Appendix B.1 we run a few misspecification tests of the original Hasbrouck model of Eq. (1), the modified model of Eq. (3), and the aggregated version of Eq. (4). We find that the MH model of Eq. (3) provides more Gaussian residuals than the original Hasbrouck model and the AMH model provides even better results. Furthermore, using the Bayesian Information Criteria (BIC), we find that the AMH model of Eq. (4) provides the best fit to the data (see the Online Appendix B.3). Consistently, we modify the latter to build a market impact model with time-varying parameters. Although the model of Eq. (4) depends on 12 parameters, in this paper, we consider a minimal modification by assuming that only  $b_0$  and  $\sigma^2$  vary through time. We define

$$\begin{aligned}\mu_t^{(1)} &:= \mu_1 + a_1 r_{t-1} + b_{0,t} x_t + b_1 x_{t-1} + \bar{b}_{10} x_t^{(10)} + \bar{b}_{100} x_t^{(100)}, \\ \mu_t^{(2)} &:= \mu_2 + c_1 r_{t-1} + d_1 x_{t-1} + \bar{d}_{10} x_t^{(10)} + \bar{d}_{100} x_t^{(100)}.\end{aligned}\tag{5}$$

Then, according to the DCS specification, we assume that  $b_{0,t}$  and  $\sigma_t^2$  follow the dynamics

$$\begin{bmatrix} b_{0,t+1} \\ \log(\sigma_{t+1}^2) \end{bmatrix} = \begin{bmatrix} \omega \\ \varrho \end{bmatrix} + \begin{bmatrix} \beta & 0 \\ 0 & \lambda \end{bmatrix} \begin{bmatrix} b_{0,t} \\ \log(\sigma_t^2) \end{bmatrix} + \begin{bmatrix} \alpha & 0 \\ 0 & \gamma \end{bmatrix} \begin{bmatrix} s_{t,1} \\ s_{t,2} \end{bmatrix},$$

where the scaled score  $s_t$  is defined in Eq. (2). We compute it from the conditional densities, that read as follows <sup>7</sup>

$$\begin{aligned}p_r(r_t | x_t, b_{0,t}, \sigma_t^2, \mathcal{F}_{t-1}, \theta) &= \frac{e^{-\frac{1}{2\sigma_t^2}(r_t - \mu_t^{(1)})^2}}{\sqrt{2\pi\sigma_t^2}}, \\ p_x(x_t | \mathcal{F}_{t-1}, \theta) &= \text{Logit}^{-1}(\mu_t^{(2)})^{\frac{1+x_t}{2}} (1 - \text{Logit}^{-1}(\mu_t^{(2)}))^{\frac{1-x_t}{2}}.\end{aligned}$$

---

<sup>7</sup>For sake of clarity, we explicitly include  $b_{0,t}$  and  $\sigma_t^2$  in the conditioning information set, even though  $b_{0,t}$  and  $\sigma_t^2$  belong to  $\mathcal{F}_{t-1}$ .

After some straightforward computations, the log-likelihood function is given by

$$\begin{aligned} \mathcal{L} := \sum_{t=1}^T \mathcal{L}_t(r_t, x_t | \mathcal{F}_{t-1}, \theta) &= -\frac{T}{2} \log 2\pi - \frac{1}{2} \sum_{t=1}^T \log \sigma_t^2 - \frac{1}{2} \sum_{t=1}^T \frac{(r_t - \mu_t^{(1)})^2}{\sigma_t^2} + \\ &\quad \sum_{t=1}^T \frac{1+x_t}{2} \log((1 + e^{-\mu_t^{(2)}})^{-1}) + \sum_{t=1}^T \frac{1-x_t}{2} \log(1 - (1 + e^{-\mu_t^{(2)}})^{-1}), \end{aligned} \quad (6)$$

thus

$$\nabla_t = \begin{bmatrix} \frac{\partial \mathcal{L}_t}{\partial b_{0,t}} \\ \frac{\partial \mathcal{L}_t}{\partial \sigma_t^2} \end{bmatrix} = \begin{bmatrix} \frac{x_t}{\sigma_t^2} (r_t - \mu_t^{(1)}) \\ \frac{(r_t - \mu_t^{(1)})^2 - \sigma_t^2}{2\sigma_t^4} \end{bmatrix} \text{ and } \mathcal{I}_{t|t-1}^{-1} = \mathbb{E}_{t-1}[\nabla_t \nabla_t^T]^{-1} = \begin{bmatrix} \sigma_t^2 & 0 \\ 0 & \sigma_t^2/2 \end{bmatrix}.$$

Hence, the dynamics of  $b_{0,t}$  is

$$b_{0,t+1} = \omega + \beta b_{0,t} + \alpha x_t (r_t - \mu_t^{(1)}), \quad (7)$$

while we restrict that of  $\log(\sigma_{t+1}^2)$  to

$$\log(\sigma_{t+1}^2) = \log(\sigma_t^2) + \gamma \left[ \frac{(r_t - \mu_t^{(1)})^2}{\sigma_t^2} - 1 \right], \quad (8)$$

where the integrated autoregressive specification is motivated by the well-known return volatility time variation at the intra-day scale (Buccheri et al. (2021)). The DCS update in Eq. (7) is the baseline autoregressive recursion for the time-varying impact parameter obtained from a general derivation. We run several tests using in-sample and out-of-sample criteria to select the most suitable DCS specification. In particular, we evaluate both stationary and integrated specifications for the DCS recursion. For selection, we rely on the BIC and the out-of-sample likelihood. The analysis reveals that for our dataset, the most suitable DCS specification is the integrated one, corresponding to  $\omega = 0$  and  $\beta = 1$ . Further

details are available in the Online Appendix B.4. In conclusion, the SDAMH model reads as

$$r_t = \mu_t^{(1)} + v_{1,t}, \quad (9)$$

$$\pi_t = \text{Logit}^{-1}(\mu_t^{(2)}), \quad (10)$$

$$b_{0,t+1} = b_{0,t} + \alpha x_t (r_t - \mu_t^{(1)}), \quad (11)$$

$$\log(\sigma_{t+1}^2) = \log(\sigma_t^2) + \gamma \left[ \frac{(r_t - \mu_t^{(1)})^2}{\sigma_t^2} - 1 \right] \quad (12)$$

where  $\mu_t^{(1)}$  and  $\mu_t^{(2)}$  are defined in Eq. (5) and  $v_{1,t} \sim N(0, \sigma_t^2)$ . The interpretation of the score-driven update of Eq. (11) is enlightening. The update of the instantaneous impact coefficient  $b_{0,t}$  is proportional to the difference between the observed return ( $r_t$ ) and the expected return <sup>8</sup> ( $\mu_t^{(1)}$ ). Then, suppose a buy market order arrives at time  $t$  ( $x_t = +1$ ). If the observed return  $r_t$  is larger than the conditional expectation  $\mu_t^{(1)}$ , one concludes that the market is less liquid than originally thought and the estimation of the instantaneous impact should be increased, i.e.  $b_{0,t+1} > b_{0,t}$ . In the opposite case, when  $r_t$  is smaller than the conditional expectation, we have  $b_{0,t+1} < b_{0,t}$ . In other words, the score-driven update provides real-time learning of the (il)liquidity (as measured by the market impact). The adjustment of  $b_{0,t+1}$  is proportional to the “surprise” brought about by a new trade with respect to the conditional expectation based on past prices and the order flow. The speed of adjustment is given by the parameter  $\alpha$ , estimated from the data via MLE.

As mentioned above for generic DCS models, one can regard our model either as a DGP or as a filter of misspecified dynamics. When used as a DGP, it describes the market impact stochastic dynamics. One does not know the instantaneous impact parameter  $b_{0,t}$  in advance, until one randomly samples past returns and market orders. When used as a filter, after observing a sequence of prices and orders, one applies the model to dynamically learn the time-varying parameter trajectory. In the latter setting, the integrated scheme of Eq. (11) is more suitable for modeling the price impact and capturing the non-stationary

---

<sup>8</sup>Note that  $\mu_t^{(1)}$  is the conditional mean of  $r_t$  given the past information  $\mathcal{F}_{t-1}$  and  $x_t$ .

behavior, possibly due to intra-day periodicity or to news announcements. As we will show in the empirical section, the integrated scheme quickly reacts in case of abrupt changes in market conditions.

As with most DCS models, our model can be estimated using MLE. Given the vector of unknown parameter  $\theta \in \Theta \subset \mathbb{R}^D$ , we maximize the log-likelihood function in Eq. (6) to find the ML estimates  $\hat{\theta}$ , as

$$\hat{\theta} = \arg \max_{\theta \in \Theta} \sum_{t=1}^T \mathcal{L}_t(r_t, x_t | \mathcal{F}_{t-1}, \theta). \quad (13)$$

Despite being quite straightforward, some care must be devoted to the initialization of the parameters in the recursion to obtain a faster and accurate convergence to the optimal solution. In the Online Appendix C we describe in more detail the estimation scheme and the initialization procedure. We also present the results of some numerical experiments on simulated data to show the effectiveness of the initialization procedure we adopt.

## 2.1 Impulse Response Analysis

In the original Hasbrouck (1991a) paper, the SVAR modeling of the joint dynamics of returns and trades is used to compute the information content of a trade by using IRF analysis. In particular, the cumulative impulse response function (CIRF) associated with a trade of a given sign provides its information content or the long-term impact. More precisely, the IRF is defined as

$$\text{IRF}(h; \delta_x) = \mathbb{E}[r_{t+h} | r_t, x_t + \delta_x, r_{t-1}, x_{t-1}, \dots] - \mathbb{E}[r_{t+h} | r_t, x_t, r_{t-1}, x_{t-1}, \dots], \quad (14)$$

where the shock on quotes is given by  $\delta_x = +1$  and the number of periods (horizons)  $h = 1, \dots, H$  is measured in “trade time”. The CIRF is then defined as

$$\text{CIRF}(H; \delta_x) = \sum_{h=1}^H \text{IRF}(h; \delta_x). \quad (15)$$

SVAR models are linear models where  $b_0$  is a constant parameter. For this reason, the shape of the IRF at each trade horizon depends only on the estimated parameters (see for instance Lütkepohl (2005)). For instance, a Hasbrouck model of Eq. (1) with  $p = 3$  can be written in matrix form as

$$\begin{bmatrix} 1 & -b_0 \\ 0 & 1 \end{bmatrix} \begin{bmatrix} r_t \\ x_t \end{bmatrix} = \begin{bmatrix} \mu_1 \\ \mu_2 \end{bmatrix} + \begin{bmatrix} a_1 & b_1 \\ c_1 & d_1 \end{bmatrix} \begin{bmatrix} r_{t-1} \\ x_{t-1} \end{bmatrix} + \begin{bmatrix} a_2 & b_2 \\ c_2 & d_2 \end{bmatrix} \begin{bmatrix} r_{t-2} \\ x_{t-2} \end{bmatrix} + \begin{bmatrix} a_3 & b_3 \\ c_3 & d_3 \end{bmatrix} \begin{bmatrix} r_{t-3} \\ x_{t-3} \end{bmatrix} + \begin{bmatrix} v_{1,t} \\ v_{2,t} \end{bmatrix},$$

or, more compactly, as  $By_t = \mu + A_1y_{t-1} + A_2y_{t-2} + A_3y_{t-3} + v_t$ , where  $y_t = (r_t, x_t)'$ ,  $\mu = (\mu_1, \mu_2)'$  and  $v_t = (v_{1,t}, v_{2,t})'$  are two-dimensional real vectors. Premultiplying the previous equation by  $B^{-1}$ , one obtains a reduced-form VAR(3) model from which the IRF easily follows as  $\text{IRF}(h; \delta_x) = JA^h J' \delta_x$ , where  $J := [I_2, \mathbf{0}, \mathbf{0}]$  is a  $2 \times 6$  selection matrix and  $\mathbf{A}$  is the  $6 \times 6$  matrix of the companion-form VAR(1) model. It is worth noticing that for Hasbrouck's model, the IRF and thus the CIRF depend only on the estimated parameters and not on the recent history of prices and trades. On the contrary, the MH, AMH, and SDAMH models do not admit close-form solutions for the IRF, both because the models are non-linear and because in the SDAMH two parameters are time-varying. To compute the IRF, we follow the procedure of Gallant et al. (1993) and Koop et al. (1996) which use Monte Carlo simulations to evaluate the Eq. (15). Notice that, as a consequence of the nonlinearity, for constant parameter models (MH and AMH) the CIRF depends both on the estimated static parameters and the "state" of the market. The history of prices and trades affects the CIRF in each trade  $t$  and, as a consequence, it is possible to compute at each point in time the contribution of the market conditions to the CIRF. The SDAMH model of Eqs. (9), (10) and (11) take a step ahead because it is a non-linear time-varying parameter model. Therefore, the CIRF depends on the estimated static parameters, the "state" of the market, and the time-varying parameters  $b_{0,t}$  and  $\sigma_t$ . As a direct consequence, in the non-linear models (AMH and SDAMH) the CIRF at a given time is different for a buy and for a sell trade, while in the linear models (e.g., Hasbrouck) the CIRF is symmetric. In the empirical analyses below we

will make the arbitrary choice of measuring the CIRF of a buy trade, but the results can also be easily obtained for a sell trade. The procedure we adopt is as follows. We first estimate the static parameters  $\theta$  of the SDAMH model on a sample day, maximizing Eq. (13). We then obtain the filtered estimates of the time-varying parameters  $b_{0,t}$  and  $\sigma_t$ . For each trade  $t$ , we simulate  $S$  times the model, using the available information set <sup>9</sup>. Specifically, for each horizon  $h = 1, \dots, H$ , we compute conditional expectations as in Eq. (14). By doing this, we generate a series of  $T - L_2$  IRFs denoted by  $\text{IRF}_{t,h}$ . Applying Eq. (15), we determine the cumulative impulse response function indicated as  $\text{CIRF}_{t,h}$ . Finally, the series of the long-run (or permanent) value of the IRF is given by the cumulative response at the last horizon lag  $\text{CIRF}_{t,H}$  and its average across the  $S$  simulation is denoted by  $\text{LRCIRF}_t$ .

### 3 Empirical analysis

This section presents the application of the SDAMH model to real data. The aim is to show the performance of the score-driven model to capture the time-varying features of the return volatility, the instantaneous impact and, thus, the temporal variations of the information content of stock trades. In the Online Appendix A, instead, we present the results obtained with numerical simulations, where we will show the finite sample performance on Monte Carlo simulations and in filtering misspecified dynamics.

#### 3.1 Dataset

Our dataset consists of four of the most capitalized stocks in the NASDAQ market, Apple Inc., Microsoft, Amazon, and Alphabet Inc., during the entire month of June 2021 (22 trading days). For the analysis, we use high-frequency data from LOBSTER (lobsterdata.com), which provides very accurate timestamping. Table 1 shows some summary statistics of the quote mid-point return  $r_t$  and the trade indicator  $x_t$  for the four investigated stocks. The

---

<sup>9</sup>Since the aggregation of the HAR model of Corsi (2009) requires a pre-sample of  $L_2 = 100$  observations, the daily computation of the IRF starts from trade 100.



stocks have different microstructural characteristics. As we can see from the (inverse) prices' values, we have two large tick stocks (AAPL and MSFT) and two small tick stocks (AMZN and GOOG). We select these stocks to analyze how tick size affects the estimated price impact and the information content of stock trades. The chosen stocks also allow us to investigate the effect of trading activity on the price impact. Table 1 shows that the average duration (in seconds) is shorter for AAPL and MSFT than for AMZN and GOOG. For our analysis, we report results for the MSFT and AMZN tickers <sup>10</sup>.

	<b>AAPL</b>	<b>MSFT</b>	<b>AMZN</b>	<b>GOOG</b>
Price	129.790	258.780	3,365.517	2,498.621
Volume	113.700	61.338	17.773	22.986
#MO	75,787	62,456	18,956	8,801
Buy (%)	53.0 %	51.7 %	51.2%	50.9 %
Dur	0.321	0.386	1.295	2.701
Spread	1.262	1.916	69.713	71.658
Mean	$6.250 \cdot 10^{-6}$	$1.065 \cdot 10^{-5}$	$3.991 \cdot 10^{-4}$	$2,134 \cdot 10^{-4}$
Std	$3.502 \cdot 10^{-3}$	$7.056 \cdot 10^{-3}$	$1.891 \cdot 10^{-1}$	$1,739 \cdot 10^{-1}$
Sk	0.188	-0.040	0.129	0.022
Ex Kurt	13.502	29.391	12.650	23.767

Table 1: Average monthly price (\$), average monthly Volume, Number of market orders (# MO), percentage of buy MO (Buy %), duration between trades (Dur) in seconds, Bid-Ask spread (Spread) in ticks, Mean, standard deviation (Std), skewness (Sk), and excess kurtosis (Ex Kurt) of  $\Delta p_t$ . Results are monthly averages for AAPL, MSFT, AMZN, and GOOG tickers on June 2021.

### 3.2 Estimation results

Table 2 shows the estimated static parameters with  $p$  values in parentheses for the two stocks. The findings are almost common for both stocks. The estimated intercept of the first equation of the model ( $\mu_1$ ) is statistically significant, negative for MSFT and positive for AMZN, indicating the presence of a global drift in the return equation. The level of the second equation (Eq. (10)),  $\mu_2$ , is instead positive for MSFT and negative for AMZN and in both cases close to zero, indicating that unconditional buy trades are as frequent as sell

<sup>10</sup>Results for AAPL and GOOG are available upon request.

trades, consistently with Table 1. Concerning the coefficients measuring the lagged impact of the midpoint return on itself, we notice that  $a_1$  is positive for MSFT, while it is negative for AMZN, indicating in the latter case a short-term mean reversion of mid-returns. The coefficients  $b_1$ ,  $\bar{b}_{10}$ , and  $\bar{b}_{100}$  in the equation of  $r_t$  measure the lagged effect of past trades on future returns. The absolute value of the first coefficient is generally larger than the others at higher lags, and all are strongly significant, confirming that the pressure of buy/sell orders on returns is strong and persistent at a high-frequency scale. The estimated absolute values of the  $b$  coefficients are higher for the small tick stock than the corresponding of the large tick stock <sup>11</sup>, indicating that the lagged impact of trades on returns is greater for stocks with higher spread-over-price ratios. This result is in line, for example, with Wyart et al. (2008), since they found a linear relationship between the bid-ask spread and the (instantaneous) impact of market orders. The impact of the past  $r_{t-1}$  on  $x_t$  is measured by the coefficient  $c_1$ , which is negative and highly significant. This coefficient captures the adjustment of the order flow to the recent price trend, and the negative sign indicates that more buyers (sellers) enter the market when the price decreases (increases). Another important feature emerging from the estimation is the strong persistence of trade signs. The positive values of  $d_1$ ,  $\bar{d}_{10}$ , and  $\bar{d}_{100}$  reflect the positive impact of the lagged trade signs on the current one. Consistently with the well-known persistence of the order flow (see, for example, Toth et al. (2012), Toth et al. (2015), and Lillo (2021)), we confirm the strong significance of the coefficients of the aggregated signs, meaning that buy (sell) orders tend to follow buy (sell) orders. Then,  $\alpha$ , the unique static parameter of the recursion in Eq. (11), measuring the level of fluctuation of the score, is statistically significant for both stocks. A similar result holds for  $\gamma$ . These finding supports the choice of a time-varying parameter approach to model the volatility and instantaneous impact behaviors. To provide further evidence of the time variability of  $b_{0,t}$ , we apply the Lagrange Multiplier test of Calvori et al. (2017), which rejects, for both stocks, the null hypothesis of a constant  $b_0$ . Finally, the initial values of the filtered instantaneous

---

<sup>11</sup>This result holds for AAPL and GOOG, too.

impact and volatility are positive and statistically significant. We conclude by noticing that the value of the daily estimates of the static parameters is stable over time. Table 2 indeed shows that the standard deviation computed on the 22 trading days in our sample (“Std”) is very small compared to the temporal average of the parameter estimates (“Est”).

### Point estimates of SDAMH model

		MSFT				AMZN					
	Est	Std		Est	Std		Est	Std		Est	Std
$\mu_1$	$-1.465 \cdot 10^{-7}$ (0.002)	$4.072 \cdot 10^{-7}$	$\mu_2$	0.023 (0.000)	0.059	$\mu_1$	$7.739 \cdot 10^{-7}$ (0.000)	$1.570 \cdot 10^{-6}$	$\mu_2$	-0.008 (0.001)	0.068
$a_1$	0.033 (0.000)	0.024	$c_1$	-13,465 (0.001)	3,396	$a_1$	-0.090 (0.000)	0.023	$c_1$	-6,706 (0.005)	1,454
$b_1$	$8.271 \cdot 10^{-6}$ (0.000)	$7.064 \cdot 10^{-7}$	$d_1$	1.445 (0.000)	0.079	$b_1$	$9.033 \cdot 10^{-6}$ (0.000)	$2.508 \cdot 10^{-6}$	$d_1$	1.912 (0.005)	0.079
$\bar{b}_{10}$	$-1.398 \cdot 10^{-6}$ (0.000)	$6.521 \cdot 10^{-7}$	$\bar{d}_{10}$	0.374 (0.000)	0.049	$\bar{b}_{10}$	$-4.087 \cdot 10^{-6}$ (0.001)	$1.810 \cdot 10^{-6}$	$\bar{d}_{10}$	0.430 (0.008)	0.077
$\bar{b}_{100}$	$-3.472 \cdot 10^{-6}$ (0.001)	$1.194 \cdot 10^{-6}$	$\bar{d}_{100}$	0.342 (0.001)	0.094	$\bar{b}_{100}$	$-4.804 \cdot 10^{-6}$ (0.001)	$2.335 \cdot 10^{-6}$	$\bar{d}_{100}$	0.359 (0.008)	0.140
$\gamma$	$9.541 \cdot 10^{-3}$ (0.000)	$5.122 \cdot 10^{-3}$	$\sigma_0$	$5.082 \cdot 10^{-5}$ (0.000)	$2.075 \cdot 10^{-5}$	$\gamma$	$2.118 \cdot 10^{-2}$ (0.000)	$1.064 \cdot 10^{-2}$	$\sigma_0$	$8.987 \cdot 10^{-5}$ (0.000)	$1.029 \cdot 10^{-4}$
$\alpha$	$4.801 \cdot 10^{-3}$ (0.000)	$2.605 \cdot 10^{-3}$	$b_{0,0}$	$4.003 \cdot 10^{-6}$ (0.000)	$3.695 \cdot 10^{-6}$	$\alpha$	$7.241 \cdot 10^{-3}$ (0.000)	$4.859 \cdot 10^{-3}$	$b_{0,0}$	$5.130 \cdot 10^{-6}$ (0.000)	$3.458 \cdot 10^{-6}$

Table 2: Temporal daily average of the coefficients (“Est”), standard deviation computed on the 22 trading samples, and  $p$ -value (in brackets) of the estimates. Results reported for MSFT and AMZN.

### 3.3 Time-varying price impact and volatility

After the discussion on the static parameters, we illustrate the behavior of the filtered time-varying parameters  $b_{0,t}$  and  $\sigma_t$ .

Figure 1 shows the filtered  $b_{0,t}$  (black dotted line) for the entire month of June 2021 for MSFT (left panel) and AMZN (right panel). As a guide for the eye, we also report a smoothed path obtained from a moving average of the estimated parameter (green line). These panels show three main important characteristics. First, the estimated parameter seems to fluctuate around an unconditional monthly constant level. Second, the instantaneous impact shows a recurring path, corresponding to an intra-day pattern. Third and more importantly, the pattern is not constant throughout the days and the time series of  $b_{0,t}$  shows occasional spikes

and breaks away from its long-term value. An example of the latter occurred on 16 June for both stocks <sup>12</sup>. These features are consistently captured by the integrated dynamics of the SDAMH model, which can adapt quickly in case of changes in market conditions, such as structural breaks, and to describe an intra-day pattern, possibly different on different days. Figure 2 reports the time-varying volatility filtered for the same month for both stocks (left panel, MSFT, and right panel AMZN). The declining daily pattern is consistent with that observed for the return volatility in Buccheri et al. (2021), with the important difference that, in that case, the authors perform the analysis in physical time at a one-second frequency on trade price returns. The dynamics resemble  $b_{0,t}$ , showing a strong intra-day pattern and occasional spikes. Then, a natural question is whether the volatility drives the instantaneous impact or vice versa or whether both follow the dynamics of a common latent factor. We leave the answer to future investigation.

To better understand the role of the time-varying instantaneous impact in price discovery, we contrast the results with those from two constant parameter models, the AMH and a novel model that we name Aggregated Hasbrouck (AH). The latter follows by applying the lag aggregation to the Hasbrouck model. The AH model reads as

$$\begin{aligned} r_t &= \mu_1 + a_1 r_{t-1} + b_0 x_t + b_1 x_{t-1} + \bar{b}_{10} x_t^{(10)} + \bar{b}_{100} x_t^{(100)} + v_{1,t}, \\ x_t &= \mu_2 + c_1 r_{t-1} + d_1 x_{t-1} + \bar{d}_{10} x_t^{(10)} + \bar{d}_{100} x_t^{(100)} + v_{2,t}, \end{aligned} \quad (16)$$

with constant volatility parameters and is a linear model with the same number of lags of the SDAMH model. A comparison with the AH model highlights the effect of the non-linearities associated with the logit and DCS specifications, while contrasting with the AMH allows to isolate the effect of the DCS specification. We consider the dynamics for two representative days, namely MSFT on June 04, 2021, and AMZN on June 23, 2021. The top panels of Figure 3 show the temporal evolution of the time-varying parameter  $b_{0,t}$  (black dots) of the SDAMH model compared with the corresponding constant parameter  $b_0$  for the AMH (cyan

---

<sup>12</sup>16 June, 2021 is the day of the FOMC announcement which will be investigated in detail in Section 4.

dashed lines) and the AH (red solid lines) models. We notice how the time variation of  $b_{0,t}$ , modeled through integrated DCS dynamics, enlightens several unprecedented features concerning the impact of  $x_t$  on  $r_t$ . The price impact is not constant throughout the day but is high during the early hours of the day and decreases as time approaches the end of the trading activity. As mentioned previously, the impact shows occasional intra-day spikes, which could be associated with abrupt liquidity crises. Relying on Blasques et al. (2016), we compute the time-varying confidence bands for  $b_{0,t}$  using Monte Carlo simulations (dashed blue lines). The bands confirm the sizeable temporal variability of  $b_{0,t}$ . The instantaneous impact estimates associated with the constant parameter models (AMH and AH) are not suitable for capturing these dynamical features. Furthermore, we notice that the estimated values for  $b_0$  for the two constant parameter models are numerically consistent with the daily average of the filtered time-varying parameter  $b_{0,t}$ . Specifically, the estimated values of  $b_0$  and the associated standard deviation (in brackets) are: for MSFT, the AMH model estimate is  $2.314 \cdot 10^{-6}$  ( $9.719 \cdot 10^{-7}$ ) and the AH model estimate is  $2.501 \cdot 10^{-6}$  ( $9.783 \cdot 10^{-7}$ ). For AMZN, the estimate of the AMH model is  $1.184 \cdot 10^{-5}$  ( $1.530 \cdot 10^{-6}$ ) and the estimate of AH is  $1.192 \cdot 10^{-5}$  ( $1.555 \cdot 10^{-6}$ ). The daily average of the filtered  $b_{0,t}$  are equal to  $2.914 \cdot 10^{-6}$  for MSFT and to  $1.294 \cdot 10^{-5}$  for AMZN. In Figure 3 (bottom panel), we also show the filtered dynamics of  $\sigma_t$  for the same sample days and stocks.

Results for AAPL and GOOG are consistent with the above discussion, with the only exception for the instantaneous impact parameter for the AAPL stock. For few days in the sample and the AH and AMH models, the constant  $b_0$  is negative. The filtered  $b_{0,t}$  on the same days for the SDAMH model fluctuates and on average is negative. This fact should not be surprising. Thinking in terms of the AH model, which is a linear model with multiple regressors, the  $b_0$  coefficient measures the partial correlation between the current trade sign and the mid-quote return. While we expect, on average, a positive correlation between the trade direction and the price movement, the strong persistence of the order flow may force the partial correlation to become negative.

### 3.4 Conditional CIRF Analysis

As stated in the original Hasbrouck (1991a) paper, one of the objectives of the model is to calculate the information content of a trade from the LRCIRF obtained with the impulse response analysis. While this is a straightforward computation for a constant parameter SVAR, the non-linearity of the logit specification and time variability of  $b_{0,t}$  and  $\sigma_t$  in our framework require a simulation approach, as described in Section 3.4, which provides a time  $t$  conditional IRF. The crucial difference, and advantage, of our model with respect to competitors is to provide a time-varying LRCIRF that depends both on the return and trade history (because of the non-linearity from the logit and the DCS specifications) and the time variability of the instantaneous impact and return volatility. To decouple the role of the different components in  $\text{LRCIRF}_t$ , we define  $\mu_{t-1}^{(*)} \doteq \mu_t^{(1)} - b_{0,t}x_t$ , which is the mean of  $r_t$  conditional on the past return  $r_{t-1}$  and past trade signs. We refer to the quantity  $\mu_{t-1}^{(*)}$  as the *state* of the market at specific trade  $t$ . For the computation of  $\text{LRCIRF}_t$  we use the CIRF at lag  $H = 20$  averaged across  $S = 1,000$  simulations. The choice  $H = 20$  is justified by the fact that for both stocks we observe that the CIRF is approximately constant at longer horizons<sup>13</sup>. It is worth stressing that, since for the linear models the IRF does not depend on the state of the market and it is linear in the shock, computing it adding an extra buy order to a buy/sell trade is equivalent to compute it by adding an extra sell order and changing the overall sign. In contrast, because of the highly non-linear specification, for the AMH and SDAMH models the computation of the IRF depends both on the nature of the shock – a buy or a sell order – and on the state of the market – that is, whether one shocks an existing buy or sell trade. In the following analysis, we compute the LRCIRF shocking the market with a buy trade. We repeated the computation with a sell trade and verified that the overall message is not changing (while the long-term impact changes, as expected). These results are available upon request.

The middle panels of Figure 3 show the temporal evolution of the time-varying LRCIRF,

---

<sup>13</sup>To be precise, at this lag, the increase of the CIRF is smaller than 1%. See also Figure 5 showing the IRFs for the two stocks on a specific day.

i.e., in Hasbrouck’s jargon, the information content of a trade or its long-term impact. Apart from noisy fluctuations, we observe a time variation of the SDAMH LRCIRF (black dotted lines), which is partially mirrored by the dynamics of  $b_{0,t}$  in the upper panels. The reason is, of course, the non-linearity of our model, whose  $\text{LRCIRF}_t$  depends both on the time-varying  $b_{0,t}$  and on the state  $\mu_{t-1}^{(*)}$  of the market at time  $t$ . As expected, the LRCIRF implied by the AH model is constant through time. Finally, it is important noticing that the AMH LRCIRF (cyan dashed lines) varies with time and, as expected, changes conditionally on the state of the market, even though the instantaneous impact parameter  $b_0$  is constant.

To disentangle and quantify the role of the time-varying impact parameter  $b_{0,t}$  and of the state  $\mu_{t-1}^{(*)}$  on the LRCIRF, we consider the regression model:

$$\text{LRCIRF}_t = \gamma_0 + \gamma_1 b_{0,t} + \gamma_2 |\mu_{t-1}^{(*)}| + \eta_t. \quad (17)$$

We estimate the regression coefficients for each of the days in our sample for both MSFT and AMZN ticker and we report in Table 3 the average of the estimated coefficients <sup>14</sup>. Furthermore, we count the number of times that we reject the null hypothesis at the significance level 5% ( $\#\{\text{Pval} < 5\%\}$ ) and report  $R^2$ . Most of the time, the point estimates are statistically significant (see  $\#\{\text{Pval} < 5\%\}$  in Table 3). Moreover, the high  $R^2$  shows that most of the variation of the long-run CIRF is captured by the two explanatory variables. Specifically, the  $\gamma_0$  coefficient is statistically significant, as well as the other parameters  $\gamma_1$  and  $\gamma_2$ . The  $\gamma_1$  is positive, while the  $\gamma_2$  is negative <sup>15</sup>. The sign of these coefficients validates the finding that the information content of stock trade positively depends on the instantaneous impact and negatively on the state of the market. According to the regression, the information content of stock trade consists of three parts: the constant ( $\gamma_0$ ), the instantaneous impact ( $\gamma_1 b_{0,t}$ ), and the *state* of the market ( $\gamma_2 |\mu_{t-1}^{(*)}|$ ). We quantify the weight of each part by computing the

---

<sup>14</sup>The average parameter estimates are computed as  $\gamma_i := \sum_{\tau=1}^{22} \gamma_{i,\tau} / 22$ ,  $i \in \{0, 1, 2, 3\}$ , where  $\gamma_{i,\tau}$  represents the  $i$ -th coefficient estimated on day  $\tau$ . The same holds for  $R^2$ .

<sup>15</sup>Their results on the coefficients are valid also when performing a regression with only one independent variable at the time.

monthly (absolute) average of each component divided by the sum across the components. The analysis indicates that the most important term explaining the information content of stock trades is the instantaneous impact component, followed by the *state* component. The least important part is the constant. In fact, for MSFT, the term  $\gamma_1 b_{0,t}$  accounts for 60%, the term  $\gamma_2 |\mu_{t-1}^{(*)}|$  for 39 %, and the remaining  $\gamma_0$  for 1 % of the weight. Similarly, for AMZN, the weights are 60%, 38%, and 2 % (respectively). We quantify the variability of  $\text{LRCIRF}_t$  explained by the two explanatory variables using the decomposition of variance of the linear model in Eq. (17). Table 4 shows that on average the variance portion explained by the time-varying impact parameter  $b_{0,t}$  is greater than that explained by the (absolute) value of the conditional information of the state. This indicates the importance of having a market impact that varies over time to adequately account for the variability of the information content of the trade. To better understand the relation between  $b_{0,t}$  and  $\mu_{t-1}^{(*)}$ , we consider the linear model

$$b_{0,t} = \gamma_0 + \gamma_3 |\mu_{t-1}^{(*)}| + \eta_t. \quad (18)$$

The estimated coefficient  $\gamma_3$  is negative and statistically significant, indicating an inverse relation between the variables. When the absolute state  $|\mu_{t-1}^{(*)}|$  is large (small), that is, the past history of price and trades predicts a large (small) price change, the instantaneous impact of a trade  $b_{0,t}$  is small (large). This behavior is consistent with the fluctuating liquidity hypothesis first introduced in Lillo and Farmer (2004) and further investigated in Taranto et al. (2014). As a robustness check of this analysis, in the Online Appendix D we extend the regression study in two directions. First, to partially control for the high-variability of the impact and volatility during the opening and closing phases of the market, we restrict the regression to observations in the time interval from 10:30 to 16:00. The estimated coefficients align with those estimated by using the whole trading day. As a second robustness check, we consider the AMH model, which inherits non-linearity and state dependence from the logit specification but has constant instantaneous impact and volatility. By regressing the  $\text{LRCIRF}$  against  $|\mu_{t-1}^{(*)}|$ , we find, again, that the state affects the  $\text{LRCIRF}$ . These findings



further support the importance of the state in determining the information content of stock trades.

### Regression results

	MSFT				AMZN			
	$\gamma_0$	$\gamma_1$	$\gamma_2$	$\gamma_3$	$\gamma_0$	$\gamma_1$	$\gamma_2$	$\gamma_3$
Est	$8.354 \cdot 10^{-6}$	0.965	$-3.809 \cdot 10^{-2}$	-	$8.302 \cdot 10^{-6}$	1.329	$-5.544 \cdot 10^{-2}$	-
$\#\{p > 5\%\}$	4	3	1	-	3	0	4	-
$R^2$	0.545				0.411			
Est	$2.8402 \cdot 10^{-6}$	-	-	$-2.904 \cdot 10^{-3}$	$1.273 \cdot 10^{-5}$	-	-	$-1.232 \cdot 10^{-2}$
$\#\{p > 5\%\}$	0	-	-	4	0	-	-	5
$R^2$	0.362				0.382			

Table 3: Results of regressions of Eqs. (17) (top) and (18) (bottom). Temporal average of the point estimates (Est), of the number of times we do not reject the null hypothesis at 5% level  $\#\{p > 5\%\}$ , and of the  $R^2$ .

### Variance decomposition

	MSFT			AMZN		
	Var $b_{0,t}$	Var $ \mu_{t-1}^{(*)} $	Var Err	Var $b_{0,t}$	Var $ \mu_{t-1}^{(*)} $	Var Err
Est (%)	33.2	24.5	42.3	30.6	22.8	46.6
Std (%)	(9.2)	(7.0)	(14.1)	(12.5)	(6.8)	(22.5)

Table 4: Temporal average (Est) of the portions of variance decompositions of  $b_{0,t}$  (Var  $b_{0,t}$ ), of  $|\mu_t^{(1)}|$  (Var  $|\mu_{t-1}^{(*)}|$ ) and of the error part (Var Err) and daily standard deviation (Std) for MSFT and AMZN.

## 4 Event study: FOMC announcement

To highlight the ability of our model to capture in real-time the dynamics of market impact and of the information content of trade, as described by the LRCIRF, we focus the analysis on a day with pre-announced macroeconomic news. Specifically, we consider June 16, 2021, when, at 14:00, the Federal Open Market Committee released the announcement communicating decisions to implement the monetary policy stance. The most eagerly awaited one was the choice of the interest rate on reserve balances (IORB). The Board of Governors of

the Federal Reserve System voted to raise the IORB from 0.10 % to 0.15 %. In the following, we study the evolution of the CIRF and the behavior of its long-term value to this day.

#### 4.1 Long run cumulative impulse response function

Figure 4 reports the filtered dynamics of the long-term cumulative impulse response function for MSFT and AMZN on June 16, 2021. Panels (a) and (b) show the  $LRCIRF_t$  for the three competing models. The estimates of the SDAMH model (black dotted lines) are jointly affected by the conditional information at time  $t$  and by the level of the instantaneous impact parameter. We observe that the long-term impact is higher at the beginning of the day when the instantaneous impact  $b_{0,t}$  is higher (see panels (c) and (d)) and when  $\mu_{t-1}^*$  is lower (see panels (e) and (f)). In the first phase of the day, the variation of  $LRCIRF_t$  resembles the dynamics of  $b_{0,t}$ . At 14:00 the FOMC releases the news about the IORB. Consequently, the  $LRCIRF_t$  increases sharply, reaching its maximum at the announcement time, and then it declines with several upward shocks as the time approaches the end of the day. For the AMH model (cyan dashed lines), the  $LRCIRF_t$  exhibits a less pronounced but similar behavior. On the one hand, the constant impact parameter keeps the  $LRCIRF_t$  of the AMH model lower than the one of the corresponding DCS version. On the other hand, the relevance of the state (see the online Appendix D) makes the two dynamics similar and very reactive to announcements. Finally, the constant  $LRCIRF_t$  of the AH model (red lines) is much higher than the average  $LRCIRF$  of the other two models. Clearly, the standard Hasbrouck's model performs poorly on days when one expects a large variability of the trade information content (before and after the announcement) and when peaks are present (as in the FOMC day) the AH model tends to overestimate it. The non-linearity and the time variation of the instantaneous impact of the SDAMH model are better suited to capture the dynamic nature of the trade information content.

## 4.2 The shape of the CIRF

The previous analysis focused on the long-term impulse response function. This section illustrates the evolution of the CIRF during the day of the FOMC announcement as a function of the time horizon and the time of day. To highlight the variability of the cumulative impulse response at each time step  $t$  and at each horizon  $h$ , we select three different phases of the day, namely from 09:45 to 09:50 as an “opening market phase”, from 11:00 to 11:05 as a “calm market phase”, and trades from 15:50 to 15:55 as the “closing market phase”, and we compute the averaged  $\text{CIRF}_{t,h}$  estimated at each trade inside the periods considered above. Figure 5 reports the estimated  $\text{CIRF}_{t,h}$  in the three phases for the SDAMH model (black diamond lines) and the AMH model (cyan circle lines). To quantify the speed of convergence and the long-term limit of the CIRF, we fit the model

$$\text{CIRF}_{t,h} = c_t + \kappa_t e^{-\phi_t h} \quad (19)$$

for fixed  $t$ . The convergence rate, that is, the speed with which the information of a trade is impounded on the price, is measured by the parameter  $\phi_t$ . We saw above that the opening market phase is characterized by high levels of instantaneous impact, low values of the state, and thus high levels of the information content of the stock trades. The left panels of Figure 5 show that the permanent level of SDAMH tends to be higher than the level of the AMH model, and achieves faster convergence. Table 5 reports the estimated value of  $\phi_t$  and we notice that the estimate  $\phi_t$  for the score-driven model is larger than that for the static parameter model. During the calm phase, the instantaneous impact parameter is small and fluctuates around its unconditional value and the state is higher (see Figure 4). In this market situation, the structure of the CIRF is mainly affected by the state ( $\mu_{t-1}^*$ ), as the instantaneous impact can be considered constant. From the middle panels of Figure 5, we notice that the speed of convergence and the permanent level in the two models are comparable. The estimates of  $\phi_t$  in Table 5 are similar. The closing phase of the market is similar to the opening one. The

right panels of Figure 5 show that the SDAMH estimates for the long-term CIRF are higher than those of the AMH model and the speed of convergence is faster for the score-driven model (see Table 5). It appears that the SDAMH cumulative responses adapt quickly in case of different market conditions, due to the dynamics of the time-varying parameter.

### Speed of convergence estimates - I

	MSFT			AMZN		
	Opening	Calm	Closing	Opening	Calm	Closing
SDAMH	0.399 (0.082)	0.302 (0.078)	0.325 (0.076)	0.668 (0.126)	0.483 (0.203)	0.370 (0.057)
AMH	0.310 (0.055)	0.301 (0.066)	0.311 (0.089)	0.631 (0.105)	0.477 (0.211)	0.346 (0.034)

Table 5: Speed of convergence parameter  $\phi_t$  from Eq.(19) during the opening, the calm and the closing phase of the market and length of the 95% confidence bands in brackets.

We now focus our attention on the informativeness of trades around the time of the FOMC announcement (14:00) by computing the average of  $\text{CIRF}_{t,h}$  over three time intervals: from 13:55 to 13:59, at 14:00, and from 14:01 to 14:05. Figure 6 shows the results for MSFT (top panels) and AMZN (bottom panels), and Table 6 reports the estimated parameter  $\phi_t$  for all curves. Before the FOMC announcement, the LRCIRF of the SDAMH model was higher than the one of the AMH model. The long-term value of SDAMH at each  $h$  tends to be high already before the time of the announcement and has a faster adjustment speed than that of the AMH model. The same holds during the FOMC announcement (middle panels). After the announcement (right panels), the level of the SDAMH  $\text{CIRF}_h$  is still higher than the one of the AMH model, as well as its speed of adjustment. From the comparison, we conclude that the effect of the time-varying parameters  $b_{0,t}$  and  $\sigma_t$  make the score-driven model more sensitive to changes in market conditions. In fact, this is evident when comparing how the level and the speed of adjustment change during the three phases. Compared to the AMH model, the SDAMH model seems to better perceive changes in market conditions before the event, and it seems to be more sensitive to the release of the FOMC announcement during the event. After the announcement, the SDAMH estimated average value tends to adjust

(in terms of levels and speed). In a less evident way, Table 6 shows that the "speed of convergence" of the AMH model is anyway sensitive 5 minutes after the announcement when the peak of informativeness has passed.

**Speed of convergence estimates - II**

	MSFT			AMZN		
	Before	During	After	Before	During	After
SDAMH	0.703 (0.062)	0.905 (0.203)	0.732 (0.107)	0.663 (0.132)	0.828 (0.191)	0.679 (0.188)
AMH	0.652 (0.981)	0.725 (0.067)	0.710 (0.111)	0.652 (0.138)	0.678 (0.220)	0.653 (0.117)

Table 6: Speed of convergence parameter  $\phi_t$  from Eq.(19) before, during, and after the announcement and length of the 95% confidence bands in brackets.

## 5 Time-varying impact for transaction cost analysis

In this section, we present a financial application, namely the real-time estimation of transaction costs due to market impact. Consider a trader who wants to sell a large amount  $Q$  of shares over a time interval  $[0, T]$ . As typical in the optimal execution literature, we assume the trader partitions the interval in  $N$  equal size subintervals of length  $\tau = T/N$  and the number of shares traded in interval  $n$  ( $n = 1, \dots, N$ ) is denoted with  $v_n\tau$  where  $v_n$  is the trading velocity<sup>16</sup>. Clearly it is  $\sum_{n=1}^N v_n\tau = -Q$ . We assume that market impact is described by an Almgren and Chriss (2001) model, which implies that the efficient stock price at the end of the  $n$ -th interval is modeled by

$$S_{n+1} = S_n + \sigma\sqrt{\tau}\epsilon_{n+1} + \beta v_{n+1}\tau,$$

where  $\beta$  is the permanent (linear) impact coefficient and  $\epsilon_i$  are standard Gaussian variables i.i.d. Let  $X_n$  be the cash account of the trader at the end of the interval  $n$ . The Almgren-

<sup>16</sup>As customary a negative (positive) value of  $v_n$  means that the trader sells (buys) in the interval.

Chriss model postulates that its dynamics is

$$X_{n+1} = X_n - v_{n+1}S_n\tau - kv_{n+1}^2\tau.$$

In this expression,  $k$  is the (linear) temporary coefficient and represents the cost incurred by the trader because of the price concession needed to attract counterparts in a short time interval. It is straightforward to prove (see Guéant (2016)) that the expected terminal cash account for a generic execution is

$$\mathbb{E}[X_N - X_0] = QS_0 - \frac{\beta}{2}Q^2 + \frac{\beta}{2}\sum_{n=1}^N v_n^2\tau^2 - k\sum_{n=1}^N v_n^2\tau.$$

Suppose for simplicity that the trader executes a TWAP (which is also optimal if the agent is risk neutral), i.e.  $v_n = -\frac{Q}{N\tau}$ . The expected implementation shortfall

$$\mathbb{E}[X_N - X_0] - QS_0 = -Q^2\left(\frac{\beta}{2}\left(1 - \frac{1}{M}\right) + \frac{k}{T}\right) \simeq -Q^2\left(\frac{\beta}{2} + \frac{k}{T}\right).$$

From this expression, it is evident that the expected terminal cash and the expected implementation shortfall depend on the impact coefficients  $\beta$  and  $k$  which must be estimated from the data to assess the cost of a large order. The estimation of  $\beta$  is typically performed via linear regression of the mid-price change over a macroscopic time interval (e.g. 5 min) against the net order flow, defined as the difference between the volume of buy and sell market orders during the time interval (see, for example, Cartea and Jaimungal (2016)). This estimation method has two major pitfalls: (i)  $\beta$  is assumed to be constant during the period used in the regression and (ii) the method requires long estimation intervals (typically one day) to obtain reliable estimates. In the following, we show that the SDAMH model provides time-varying estimates of  $\beta$ , which can be used successfully to predict permanent impact without the need to aggregate data in physical time. To this end, consider a time interval in which  $M$  trades are executed in the market. A way of quantifying permanent impact is to estimate

the following ratio  $\hat{\beta}_t = \frac{\sum_{j=t-M}^{t-1} \Delta q_j}{\sum_{j=t-M}^{t-1} v_j}$ , where  $\Delta q_t = q_t - q_{t-1}$  is the midpoint price change and  $v_t$  the signed volume of the  $t$ -th trade. To use our model that considers trade signs, we notice that  $\hat{\beta}_t \simeq \frac{\bar{q}_t}{\bar{v}_t} \frac{\sum_{j=t-M}^{t-1} r_j}{\sum_{j=t-M}^{t-1} x_j} = \frac{\bar{q}_t}{\bar{v}_t} \hat{\beta}_t^{(s)}$ , where  $\bar{q}_t$  and  $\bar{v}_t$  are, respectively, the average midpoint price and the average absolute trading volume in the interval. In the above equation, we have introduced the quantity (the superscript  $(s)$  stands for trade sign)

$$\hat{\beta}_t^{(s)} := \frac{\sum_{j=t-M}^{t-1} r_j}{\sum_{j=t-M}^{t-1} x_j}. \quad (20)$$

The estimator requires the aggregation of  $M$  events and might be highly fluctuating especially when the denominator is close to zero, i.e. when the number of buy and sell trades is approximately the same. For these reasons, it is customary to estimate the permanent impact by performing a linear regression of the aggregate price change versus the aggregate order flow in a longer time window, such as a day (as in Cartea and Jaimungal (2016)). The SDAMH model, instead, provides an estimation that is updated at each trade, does not require event aggregation, and avoids the high fluctuations for approximately balanced markets. In Online Appendix E we show that if the data follows an SDAMH model, the estimator of the time-varying impact coefficient is approximated by

$$\hat{\beta}_t^{(s)} \simeq \frac{\bar{b}_{0,t} + b_1 \omega_t^{(1)} + \bar{b}_{10} \omega_t^{(L_1)} + \bar{b}_{100} \omega_t^{(L_2)}}{1 - a_1}, \quad (21)$$

where  $\bar{b}_{0,t}$  is the local average of the instantaneous impact estimated from trade  $t - M$  to  $t - 1$  and  $\omega_t^{(1)}$ ,  $\omega_t^{(L_1)}$ , and  $\omega_t^{(L_2)}$  are local averages of the trade signs in the same interval (see Online Appendix E for details). Finally, the estimator of the time-varying permanent impact coefficient reads

$$\hat{\beta}_t \simeq \frac{\bar{q}_t}{\bar{v}_t} \frac{\bar{b}_{0,t} + b_1 \omega_t^{(1)} + \bar{b}_{10} \omega_t^{(L_1)} + \bar{b}_{100} \omega_t^{(L_2)}}{1 - a_1}. \quad (22)$$

Clearly,  $\bar{q}_t$  and  $\bar{v}_t$  can be also computed with a local estimation using, for example, an EWMA <sup>17</sup>. Eq. (22) depends both on instantaneous impact and on the *state* of the market. The final expression for  $\hat{\beta}_t^{(s)}$  is consistent with the findings of this work: The permanent impact positively depends on the instantaneous impact parameter, through  $\bar{b}_{0,t}$ , and negatively on the state, through the  $\omega_t$ 's coefficients. In the absence of the *state* coefficients, the lagged impacts of the order flow on the permanent impact are directly measured by the  $b_1$ ,  $\bar{b}_{10}$  and  $\bar{b}_{100}$ . The coefficients of  $\omega_t$ 's can be interpreted as factors that weigh the effect of the change in the *state* of the market on the permanent impact. For example, consider  $\omega_t^{(1)} := \bar{x}_{t-1}/\bar{x}_t$ , where  $\bar{x}_t$  is the average of the trade signs in the interval  $[t - M, t - 1]$ . We have that if the number of buy orders is higher than that in the previous interval (i.e.  $\bar{x}_t > \bar{x}_{t-1}$ ), the order flow tends to be unbalanced by the increasing pressure of buy orders. The coefficient  $\omega_t^{(1)}$  describes the change in the *state* of the market and the effect on the permanent impact coefficient:  $b_1$  is weighed by  $\omega_t^{(1)} < 1$ , which produces a reduction in the permanent impact coefficient. In contrast, the order flow tends to be unbalanced by the increasing pressure of sell orders. The coefficient  $b_1$  is weighed by  $\omega_t^{(1)} > 1$ , which produces an increase in the permanent impact coefficient. The same holds for  $\omega_t^{(L_1)}$  and  $\omega_t^{(L_2)}$ .

To validate our estimator, in the Online Appendix E.2 we present a Monte Carlo experiment showing that the SDAMH approach provides estimates of the permanent impact coefficient consistent with those of a regression approach on aggregated data. This result supports the reliability of the SDAMH approach to estimate the permanent impact. Moreover, the full exploitation of tick-by-tick returns and trade-sign data allows us to obtain estimates with low error bands of the permanent impact coefficient in simulations.

We now present an application to real data. We compare the out-of-sample performance in estimating the permanent impact when using the two approaches. For this, we compute today's estimates of the permanent impact using coefficients estimated on the previous day.

---

<sup>17</sup>Alternatively, one could develop a score-driven Hasbrouck model where the first variable is the mid-point price change  $\Delta q_t$  (instead of the return  $r_t$ ) and the second variable is the signed volume  $v_t$  (instead of the trade sign  $x_t$ ). We leave this extension for future work.



Specifically, we first obtain parameter estimates from the previous day for the DCS model. Then, we filter the time-varying instantaneous impact dynamics using today’s observation in an online mode, and we calculate the impact using the equation (22) with an aggregation window of  $M = 101$  trades. Taking into account the average duration (see Table 1), 1,000 trades roughly coincide with the first 5 minutes of trading. This window is wide enough for the initialization method to be effective. In this approach, the permanent impact estimation is conditional on the information flow of the day of the forecast. For the regression approach, we compute the estimate on the previous day’s data, by regressing the one minute<sup>18</sup> returns versus the contemporaneous net order flow (in this case the difference between the number of buyer and seller-initiated trades). In the end, we use the estimate as an unconditional prediction for the actual day. Figure 7 shows the estimated  $\hat{\beta}_t^{(s)}$  for the two days investigated. For both samples, we observe clear dynamics of the permanent impact coefficient. We notice that the estimated time-varying  $\hat{\beta}_t^{(s)}$  tends to fluctuate around  $\hat{\beta}^{(reg)}$  but many observations lie outside the confidence bands estimated using OLS. Comparing the temporal average of  $\hat{\beta}_t^{(s)}$  and  $\hat{\beta}^{(reg)}$ , we notice that the two approaches provide quite different point estimates: we have that their relative absolute difference is roughly 30% for both MSFT and AMZN. To statistically verify the difference between the two, we performed a t-test on the 22 days of the sample. The rejection of the null hypothesis of the t-test performed on the series of permanent impacts for both stocks makes us better realize the out-of-sample gap between the two approaches.

The significance of the difference between the time-varying  $\hat{\beta}_t^{(s)}$  and the constant  $\hat{\beta}^{(reg)}$  can be better appreciated by quantifying the error on the first. To this end, we rely on the method of Blasques et al. (2016) to estimate the uncertainty of the parameters in score-driven models by computing confidence bands of a parameter that varies over time ( $b_{0,t}$  in our case, as in Figure 3) using Monte Carlo simulations. Then, by the propagation of errors, we compute confidence bands of the  $\hat{\beta}_t^{(s)}$  for the SDAMH model. Our calculations show that

---

<sup>18</sup>We use aggregated data over 1 minute to be consistent with the choice of  $M = 101$  (see average duration (Dur) in Table 1) transactions used for the SDAMH approach.

the width of the confidence bands is, on average,  $4.125 \cdot 10^{-6}$  for MSFT and  $1.561 \cdot 10^{-5}$  for AMZN, that is, significantly smaller than the variability range of  $\hat{\beta}_t^{(s)}$ . In conclusion, it is evident that the estimated permanent impact varies considerably throughout the day and a regression estimation based on the entire trading day would not be able to capture this variability, leading to severe mis-estimation of transaction costs.

## 6 Conclusions

The groundbreaking paper of Hasbrouck (1991a) pioneered and continues to drive research on trade information content. In the original specification, the mid-quote price change and the trade sign follow the joint dynamics described by an SVAR model. The literature has later highlighted a few drawbacks of this approach: the model for trade signs can be severely miss-specified; estimates can be contradictory when the permanent impact function has a non-linear relationship with the trade sign; to capture the long memory of the order flow, the model needs parsimony. The most severe pitfall is the assumption that the instantaneous impact, a quantity inversely related to market liquidity, is constant. Recent research shows that liquidity fluctuates highly in time and shows strong intra-day patterns (Cont et al. (2014); Mertens et al. (2021)). This paper proposes a new approach to fix these pitfalls. First, we do not model price changes and trade signs, but mid-quote price returns jointly with the *probability* of the occurrence of a buy trade. We adopt a specification based on the logistic function, which introduces some non-linearity in the approach. As a relevant outcome of this specification, the long-term behavior of the trade impact, as measured by the CIRF, depends on the local state of the market, marking a crucial difference from the linear specification of Hasbrouck. Second, we ensure a parsimonious description of the order-flow dynamics by adapting to the present context the heterogeneous specification introduced in Corsi (2009) to model the realized volatility. The effect on our modeling approach is two-fold: we can capture very long persistence in terms of very few parameters, and the aggregation over

the different time scales significantly improves the quality of the specification, as measured by several statistics applied to the model's residuals. Then, to adequately describe the empirical behavior of market liquidity and volatility, we assume that the instantaneous impact coefficient and return volatility follow observation-driven dynamics in the spirit of the score-driven approach by Creal et al. (2013) and Harvey (2013). We name the novel approach the Score-Driven Aggregated Modified Hasbrouck (SDAMH) model. We test the model on actual data by exploiting a sample of trades and quotes for AAPL, MSFT, AMZN, and GOOG stocks from the NASDAQ market in June 2021. In the main text, we report the results for MSFT and AMZN.

The outcome of the empirical exercise is convincing, robust, and has important implications. i) After estimation, which is straightforward and based on the standard maximum likelihood approach, the model adequately captures the liquidity's and volatility's intraday time variation. ii) The instantaneous impact reacts quickly to changing market conditions, as documented in the investigation of the liquidity behavior on FOMC announcement days. iii) The permanent market impact measured by the CIRF strongly depends on the instantaneous time-varying impact level and the market's state. Hasbrouck's original specification cannot capture both effects.

In the paper's final section, we investigate the connection between the SDAMH model and the regression approach (see, for instance, Cartea and Jaimungal (2016)) to estimate the permanent impact parameter in a transaction cost analysis problem. We show that on a daily scale, our approach provides an estimate consistent with that based on the regression. However, since we do not need to aggregate the data as in the regression approach, we can exploit the complete information from the tick-by-tick time series, potentially resulting in a more accurate estimation. Moreover, our approximate closed-form expression for the permanent impact parameter crucially depends on the time-varying impact parameter and the market state. We foresee several possible extensions of this work. First, one can modify the model using trade volume rather than signs. A model with time-varying  $b_0$ , which

realistically describes the liquidity's fluctuating and adaptive nature, is mandatory to design new optimal execution strategies. Finally, we have only considered the instantaneous impact and the volatility as time-varying. Still, one can extend the SDAMH to the case where the parameters describing the role of past quotes and trades on market impact, and thus the "memory" of the market, are time-varying.

# References

- Agresti, A. (2015). *Foundations of linear and generalized linear models*. John Wiley & Sons.
- Almgren, R. and Chriss, N. (2001). Optimal execution of portfolio transactions. *Journal of Risk*, 3:5–40.
- Barclay, M. J., Hendershott, T., and McCormick, D. T. (2003). Competition among trading venues: Information and trading on electronic communications networks. *The Journal of Finance*, 58(6):2637–2665.
- Blasques, F., Koopman, S. J., Lasak, K., and Lucas, A. (2016). In-sample confidence bands and out-of-sample forecast bands for time-varying parameters in observation-driven models. *International Journal of Forecasting*, 32(3):875–887.
- Bollerslev, T. (1986). Generalized autoregressive conditional heteroskedasticity. *Journal of Econometrics*, 31(3):307–327.
- Bouchaud, J.-P., Bonart, J., Donier, J., and Gould, M. (2018). *Trades, quotes and prices: financial markets under the microscope*. Cambridge University Press.
- Bouchaud, J.-P., Farmer, J. D., and Lillo, F. (2009). How markets slowly digest changes in supply and demand. In *Handbook of financial markets: dynamics and evolution*, pages 57–160. Elsevier.
- Bouchaud, J.-P., Gefen, Y., Potters, M., and Wyart, M. (2003). Fluctuations and response in financial markets: the subtle nature of random price changes. *Quantitative Finance*, 4(2):176.
- Buccheri, G., Bormetti, G., Corsi, F., and Lillo, F. (2021). A score-driven conditional correlation model for noisy and asynchronous data: An application to high-frequency covariance dynamics. *Journal of Business & Economic Statistics*, 39(4):920–936.
- Calvori, F., Creal, D., Koopman, S. J., and Lucas, A. (2017). Testing for parameter instability across different modeling frameworks. *Journal of Financial Econometrics*, 15(2):223–246.
- Cartea, A. and Jaimungal, S. (2016). Incorporating order-flow into optimal execution. *Mathematics and Financial Economics*, 10(3):339–364.
- Cont, R., Kukanov, A., and Stoikov, S. (2014). The price impact of order book events. *Journal of Financial Econometrics*, 12(1):47–88.
- Corsi, F. (2009). A simple approximate long-memory model of realized volatility. *Journal of Financial Econometrics*, 7(2):174–196.
- Creal, D., Koopman, S. J., and Lucas, A. (2013). Generalized autoregressive score models with applications. *Journal of Applied Econometrics*, 28(5):777–795.
- Dufour, A. and Engle, R. F. (2000). Time and the price impact of a trade. *The Journal of Finance*, 55(6):2467–2498.
- Dufour, A. and Nguyen, M. (2012). Permanent trading impacts and bond yields. *The European Journal of Finance*, 18(9):841–864.
- Engle, R. F. and Gallo, G. M. (2006). A multiple indicators model for volatility using intra-daily data. *Journal of Econometrics*, 131(1-2):3–27.
- Engle, R. F. and Patton, A. J. (2004). Impacts of trades in an error-correction model of quote prices. *Journal of Financial Markets*, 7(1):1–25.
- Engle, R. F. and Russell, J. R. (1998). Autoregressive conditional duration: a new model for irregularly spaced transaction data. *Econometrica*, pages 1127–1162.

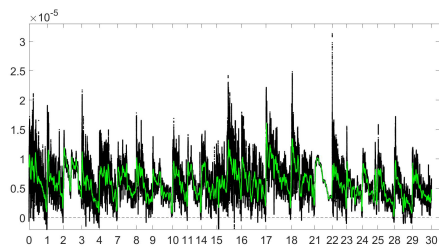
- Gallant, A. R., Rossi, P. E., and Tauchen, G. (1993). Nonlinear dynamic structures. *Econometrica: Journal of the Econometric Society*, pages 871–907.
- Gillemot, L., Farmer, J. D., and Lillo, F. (2006). There’s more to volatility than volume. *Quantitative Finance*, 6(5):371–384.
- Glosten, L. R. and Milgrom, P. R. (1985). Bid, ask and transaction prices in a specialist market with heterogeneously informed traders. *Journal of Financial Economics*, 14(1):71–100.
- Guéant, O. (2016). *The Financial Mathematics of Market Liquidity: From optimal execution to market making*, volume 33. CRC Press.
- Harvey, A. C. (2013). *Dynamic models for volatility and heavy tails: with applications to financial and economic time series*, volume 52. Cambridge University Press.
- Hasbrouck, J. (1988). Trades, quotes, inventories, and information. *Journal of Financial Economics*, 22(2):229–252.
- Hasbrouck, J. (1991a). Measuring the information content of stock trades. *The Journal of Finance*, 46(1):179–207.
- Hasbrouck, J. (1991b). The summary informativeness of stock trades: An econometric analysis. *The Review of Financial Studies*, 4(3):571–595.
- Hasbrouck, J. (2007). *Empirical market microstructure: The institutions, economics, and econometrics of securities trading*. Oxford University Press.
- Hasbrouck, J. (2021). Price discovery in high resolution. *Journal of Financial Econometrics*, 19(3):395–430.
- Hautsch, N. and Huang, R. (2012). The market impact of a limit order. *Journal of Economic Dynamics and Control*, 36(4):501–522.
- Koop, G., Pesaran, M. H., and Potter, S. M. (1996). Impulse response analysis in nonlinear multivariate models. *Journal of Econometrics*, 74(1):119–147.
- Kyle, A. S. (1985). Continuous auctions and insider trading. *Econometrica: Journal of the Econometric Society*, pages 1315–1335.
- Lillo, F. (2021). Order flow and price formation. *arXiv preprint arXiv:2105.00521*.
- Lillo, F. and Farmer, J. D. (2004). The long memory of the efficient market. *Studies in nonlinear dynamics & econometrics*, 8(3).
- Lütkepohl, H. (2005). *New introduction to multiple time series analysis*. Springer Science & Business Media.
- Mertens, L. P., Ciacci, A., Lillo, F., and Livieri, G. (2021). Liquidity fluctuations and the latent dynamics of price impact. *Quantitative Finance*, pages 1–21.
- Nelson, D. B. et al. (1996). Asymptotically optimal smoothing with arch models. *Econometrica*, 64(3):561–573.
- O’Hara, M. (2003). Presidential address: Liquidity and price discovery. *The Journal of Finance*, 58(4):1335–1354.
- Philip, R. (2020). Estimating permanent price impact via machine learning. *Journal of Econometrics*, 215(2):414–449.

- Taranto, D. E., Borometti, G., and Lillo, F. (2014). The adaptive nature of liquidity taking in limit order books. *Journal of Statistical Mechanics: Theory and Experiment*, 2014(6):P06002.
- Toth, B., Eisler, Z., Lillo, F., Kockelkoren, J., Bouchaud, J.-P., and Farmer, J. D. (2012). How does the market react to your order flow? *Quantitative Finance*, 12(7):1015–1024.
- Toth, B., Palit, I., Lillo, F., and Farmer, J. D. (2015). Why is equity order flow so persistent? *Journal of Economic Dynamics and Control*, 51:218–239.
- Wyart, M., Bouchaud, J.-P., Kockelkoren, J., Potters, M., and Vettorazzo, M. (2008). Relation between bid–ask spread, impact and volatility in order-driven markets. *Quantitative finance*, 8(1):41–57.

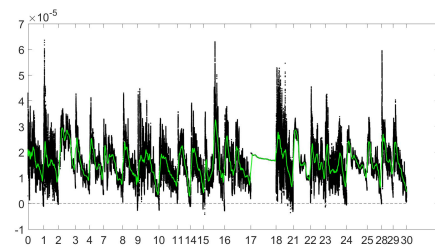
# Figures



## All sample time-varying estimates of the instantaneous impact



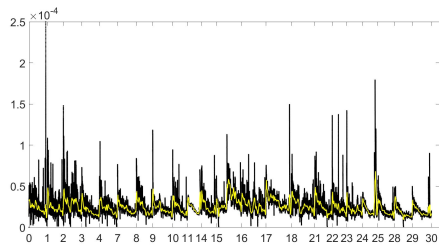
(a) June, 2021 - MSFT



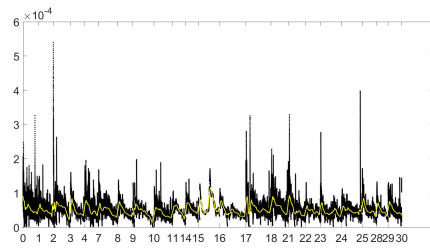
(b) June, 2021 - AMZN

Figure 1: Estimates of the time-varying instantaneous impact parameter of the SDAMH model (black lines) and its moving average (green solid lines). Overview of June 2021 trading month.

## All sample time-varying estimates of the volatility



(a) June, 2021 - MSFT



(b) June, 2021 - AMZN

Figure 2: Estimates of the time-varying volatility of the SDAMH model (black lines) and its moving average (yellow solid lines). Overview of June 2021 trading month.

# Online supplementary material

## Appendix A Monte Carlo study

In this appendix, we present the finite-sample performance of MLE on data generated according to the SDAMH model and the results obtained when it is used as a filter of misspecified (and non-stationary) dynamics.

### A.1 Finite sample performance of MLE on simulations

We first perform a Monte Carlo experiment to investigate the statistical properties of the MLE of the vector of static parameter  $\theta$ , when the DGP is our model. The procedure is the following: 1. Simulate the time series of  $T = 10,000$  observations from Eqs. (9), (10) and (11) for values of the static parameter vector (see the first column of Table 7, "Par") close to the estimates we obtain using real data (see Table 2), 2. Estimate the model, maximizing the log-likelihood function in Eq. (6) according to the procedure C.1, 3. Repeat 1) and 2)  $S = 100$  times, 4. Collect the  $S$  estimates to compute summary statistics. As Table 7 suggests, the MLE can identify point estimates very close to the true values when the DGP is our model. The results are homogeneous in almost all coefficient estimates. The standard deviation in the simulation is low with respect to both the mean and the median. Moreover, the low quantile simulation range indicates that the coefficients are correctly identified.

### A.2 Filtering a misspecified dynamics

This section shows the ability of the SDAMH model as a predictive filter Nelson et al. (1996) of misspecified dynamics. Specifically, we simulate a model described by Eqs. (9) and (10), but the dynamics of the parameter  $b_{0,t}$  is not described by Eq. (11), but follows a different specification. More precisely, we test three deterministic and one stochastic dynamics of the parameter  $b_{0,t}$ , namely: 1. **Fast Sine**  $b_{0,t+1}^* = 0.5 + 0.5 \sin(2\pi t/200)$ , 2. **Step**  $b_{0,t+1}^* = \mathbb{I}(t > 500)$ , 3. **Ramp**  $b_{0,t+1}^* = \text{mod}(t/200)$ , 4. **AR(1)**  $b_{0,t+1}^* = c + \phi b_{0,t}^* + u_t$  with  $c = 0.05$  and  $\phi = 0.9$ . We then use our model to filter the generated paths of the time-varying

### Monte Carlo simulations of MLE finite sample performance

Par	True	Mean	Median	Std	$\Delta q$
$\mu_1$	$-1.465 \cdot 10^{-7}$	$-1.473 \cdot 10^{-7}$	$-1.471 \cdot 10^{-7}$	$5.113 \cdot 10^{-8}$	$1.747 \cdot 10^{-7}$
$\mu_2$	$2.325 \cdot 10^{-2}$	$2.335 \cdot 10^{-2}$	$2.324 \cdot 10^{-2}$	$3.045 \cdot 10^{-3}$	$5.088 \cdot 10^{-3}$
$a_1$	$3.384 \cdot 10^{-2}$	$3.379 \cdot 10^{-2}$	$3.388 \cdot 10^{-2}$	$1.722 \cdot 10^{-3}$	$3.133 \cdot 10^{-3}$
$b_1$	$8.271 \cdot 10^{-6}$	$8.275 \cdot 10^{-6}$	$8.277 \cdot 10^{-6}$	$8.387 \cdot 10^{-8}$	$2.686 \cdot 10^{-7}$
$c_1$	-1,3470	-1,3490	-1,3480	109	513
$d_1$	1.445	1.444	1.445	$1.024 \cdot 10^{-2}$	$3.196 \cdot 10^{-2}$
$\bar{b}_{10}$	$8.271 \cdot 10^{-6}$	$8.275 \cdot 10^{-6}$	$8.277 \cdot 10^{-6}$	$8.387 \cdot 10^{-8}$	$2.686 \cdot 10^{-7}$
$\bar{d}_{10}$	0.374	0.373	0.374	$1.643 \cdot 10^{-2}$	$4.766 \cdot 10^{-2}$
$\bar{b}_{100}$	$-3.472 \cdot 10^{-6}$	$-3.475 \cdot 10^{-6}$	$-3.485 \cdot 10^{-6}$	$1.504 \cdot 10^{-7}$	$4.733 \cdot 10^{-7}$
$\bar{d}_{100}$	0.342	0.342	0.342	$2.754 \cdot 10^{-2}$	$4.161 \cdot 10^{-2}$
$\alpha$	$4.802 \cdot 10^{-3}$	$2.807 \cdot 10^{-3}$	$3.804 \cdot 10^{-3}$	$2.399 \cdot 10^{-4}$	$5.176 \cdot 10^{-4}$
$b_{0,0}$	$4.003 \cdot 10^{-6}$	$4.003 \cdot 10^{-6}$	$4.005 \cdot 10^{-6}$	$2.043 \cdot 10^{-7}$	$4.679 \cdot 10^{-7}$
$\gamma$	$9.542 \cdot 10^{-3}$	$9.547 \cdot 10^{-3}$	$9.544 \cdot 10^{-3}$	$3.406 \cdot 10^{-4}$	$9.965 \cdot 10^{-4}$
$\sigma_0$	$5.083 \cdot 10^{-5}$	$5.087 \cdot 10^{-5}$	$5.082 \cdot 10^{-5}$	$1.737 \cdot 10^{-6}$	$5.870 \cdot 10^{-6}$

Table 7: True value of the parameters (True), mean, median, standard deviation (Std) and the difference between the quantile at 95% and the quantile at 5% ( $\Delta q$ ) estimated using Monte Carlo simulations.

parameter from the observations of  $x_t$  and  $r_t$  and we evaluate its performances by comparing with the true parameter dynamics. The Monte Carlo study is carried out using a sample size  $T$  of 10,000 observations and  $S = 100$  simulated paths<sup>19</sup>. Figure 8 shows the simulated trajectories of  $b_{0,t}$  (solid red line) together with the time series filtered using the SDAMH model (black dots) for the  $S = 1,000$  Monte Carlo replicas. The filtered paths follow quite closely the true parameter dynamics, even if the DGP is not an SDAMH model. Moreover, the filtered paths are capable of tracing and capturing abrupt changes of  $b_{0,t}^*$ . Despite its integrated nature, the filter can also reproduce a misspecified stationary trajectory as shown in panel (d). To quantify the accuracy of the model in capturing the behaviors of  $b_{0,t}^*$ , we compute the Mean Absolute Error (MAE), defined as  $\text{MAE}(b_{0,t}) = \frac{1}{T} \sum_{t=1}^T |b_{0,t} - b_{0,t}^*|$ . To consider a relative measure of deviation between the simulated and filtered path, we divide the MAE by the absolute value of the average of the simulated path ( $|\bar{b}_{0,t}^*|$ ). This quantity is named MAE\*, and is computed as:  $\text{MAE}^* = \frac{1}{|\bar{b}_{0,t}^*|} \text{MAE}$ . We then compute the average over

<sup>19</sup>For the AR(1) process, we generate only one sample of  $b_{0,t}$ , but 100 simulations of the  $(r_t, x_t)$  process.

the  $S$  simulations using two different sample sizes:  $T = 1,000$  and  $T = 10,000$ . The results are reported in Table 8. These results show that the SDAMH works well in recovering the true pattern of the time-varying parameter and it can be considered an effective filter also for stochastic autoregressive processes, although in the case of stationary AR(1) process, the error is larger. This is consistent with the nonstationary characteristic of the SDAMH filter. Interestingly, in all cases, the MAE clearly shrinks as the sample size increases.

<b>Relative Mean Absolute Error on MCs</b>					
	T	Fast Sine	Step	Ramp	AR(1)
MAE*	1,000	0.178	0.220	0.216	0.251
MAE*	10,000	0.085	0.093	0.89	0.103

Table 8: Mean Absolute Error divided by  $|\bar{b}_{0,t}|$  ( $\text{MAE}^*(b_{0,t})$ ) of the filtered paths averaged over the number of Monte Carlo simulations for two different sample size:  $T = 1,000$  and  $T = 10,000$ .

## Appendix B Model comparison and selection

This appendix compares different models and selects the best one. Our comparison criterion is based on the skewness, kurtosis, and homoscedasticity of residuals, while the model selection is based on the Bayesian Information Criterion (BIC). We also compare the integrated and stationary specifications of the instantaneous impact DCS dynamics. The considered models are (i) the original Hasbrouck (H) model of Eq. (1) with  $p = 5$  lags, (ii) the modified Hasbrouck (MH) model of Eq. (3) with  $p = 5$  lags, (iii) the AMH model of Eq. (4), and (iv) the SDAMH model of Eqs. (9), (10), and (11). For illustrative purposes, we report results only for two sample days for MSFT and AMZN.

### B.1 Residuals diagnostic: skewness and kurtosis

In this part, we compute the skewness and kurtosis of the residuals to test whether the distributions of the data are far from the Gaussian assumption. For the residuals of the return equation we consider standardized residuals, whereas for the trade sign equation, we

test quantile residuals. The reason is that in this case, we have residuals from an inverse logistic and, thus, of a generalized linear model (see Agresti (2015) for more details). In the original H model, we test directly the residuals, since this is a linear model.

Tables 9 and 10 show the results. For the return equation, since the skewness and the kurtosis of the original Hasbrouck’s model are far from the Gaussian ones, we conclude that the model is highly misspecified. The inverse logistic transformation improves the residuals of the trade sign in the case of the MH model. The use of the aggregation technique (jointly with the non-linear transformation) strongly improves the quality of the results, but some issues are still present for the  $r_t$  equation. Finally, with the introduction of the time-varying parameters in the SDAMH model, the analysis can be considered satisfactory.

<b>Skewness</b>				
	<b>MSFT</b>		<b>AMZN</b>	
	$r_t$	$x_t$	$r_t$	$x_t$
H	-0.274	-0.074	0.131	0.108
MH	-0.134	0.020	0.132	-0.020
AMH	-0.076	0.013	0.081	0.021
SDAMH	-0.010	0.012	0.026	-0.016

Table 9: Skewness of the standardized residuals of the return equation for the four investigated models, skewness of the standardized residuals of the trade sign equation for the H model, and the skewness of the quantile residuals for the remaining three models. Results for MSFT on June 04, 2021, and AMZN on June 23, 2021.

## B.2 Residuals diagnostic: homoscedasticity test

To test whether our model is well specified, we perform a Lagrange Multiplier (LM) test with  $p = \{1, 2, 3, 4, 5, 7, 10, 15, 20, 50\}$  lags and, for each model, we report in Table 11 the number of times the null hypothesis of homoscedastic residuals is not rejected. For the non-linear models (AMH and SDAMH), we test the quantile residuals of the trade sign equation. The test shows that, while residuals of the Hasbrouck’s and the AH model are heteroscedastic, especially for the return variable, the picture improves after lag aggregation and the non-

<b>Kurtosis</b>				
	<b>MSFT</b>		<b>AMZN</b>	
	$r_t$	$x_t$	$r_t$	$x_t$
H	17.352	3.708	9.368	5.787
MH	10.809	3.488	8.554	3.599
AMH	8.420	3.255	7.373	3.421
SDAMH	3.467	3.104	3.538	2.956

Table 10: Kurtosis of the standardized residuals of the return equation for the four investigated models, kurtosis of the standardized residuals of the trade sign equation for the H model, and the kurtosis of the quantile residuals for the remaining three models. Results for MSFT on June 04, 2021, and AMZN on June 23, 2021.

linear transformation in the AMH model. The residual homoscedasticity hypothesis cannot be rejected for the DCS version where  $b_{0,t}$  and  $\sigma_t^2$  are time-varying. This strengthens the conclusion that our model is better specified than Hasbrouck’s one.

#### **Results of a Lagrange Multiplier test on residuals**

	<b>MSFT</b>		<b>AMZN</b>	
	$r_t$	$x_t$	$r_t$	$x_t$
H	0	5	0	5
AH	1	6	2	4
AMH	3	10	3	6
SDAMH	9	10	8	10

Table 11: Number of times the null hypothesis is not rejected at 5% for the LM test with lags  $p = \{1, 2, 3, 4, 5, 7, 10, 15, 20, 50\}$  on the residual equations for MSFT June 04, 2021 and AMZN on June 23, 2021.

Table 11 shows the results of the homoscedasticity test for two days from the sample and two stocks, MSFT and AMZN. An interesting related analysis concerns the homoscedasticity test on aggregated residuals. We consider both aggregations on 100 consecutive transactions and on a minute of physical time. Table 12 summarized the results and confirms that the SDAMH model provides homoscedastic aggregated residuals, pointing to the fact that a joint mid-quote return and trade sign model should account for liquidity and volatility time-variation (while, of course, the Hasbrouck’s model cannot). It is worth mentioning that the idea that volatility clustering is related to the persistence of market impact and not to the



clustering of volume or several trades has been proposed in Gillemot et al. (2006) by using surrogate data analysis.

### Results of LM test on aggregated residuals

	100 trades				1 minute			
	MSFT		AMZN		MSFT		AMZN	
	$r_t$	$x_t$	$r_t$	$x_t$	$r_t$	$x_t$	$r_t$	$x_t$
H	0	0	1	3	10	9	8	8
AH	0	5	0	4	8	4	8	9
AMH	2	10	2	10	7	10	7	10
SDAMH	9	10	7	10	9	10	7	10

Table 12: Number of times the null hypothesis cannot be rejected at 5% for the LM test with lags  $p = \{1, 2, 3, 4, 5, 7, 10, 15, 20, 50\}$  residuals aggregated over 100 trades (left) and 1 minute (right) for MSFT 04 June, 2021 and AMZN on 23 June, 2021.

### B.3 Model selection among constant parameter models

In this section, we perform a model selection on the three constant parameter models (H, AH, and AMH) by using the Bayesian Information Criterion, defined as

$$BIC = K \log(T) - \log(\hat{\mathcal{L}}), \quad (23)$$

where  $K$  is an integer indicating the number of model parameters,  $T$  is the length of the time series, and  $\hat{\mathcal{L}}$  is the overall maximized likelihood function. Instead of reporting the value of the estimated BIC on each of the 22 sample days for MSFT and AMZN, we report in Table 13 the number of times (days) the BIC of one of the proposed models is better than the others. We observe that the AMH model is better than both the H and AH models. In the range of 77-82 % days, the model with the aggregation of lags overcomes the other two constant-parameter models. This shows that aggregation is a key element for better modeling of joint price and trade dynamics.

## Results of BIC on different static parameter models

	MSFT		AMZN	
H	2	9.1 %	2	9.1 %
AH	3	13.6 %	2	9.1 %
AMH	17	77.4 %	18	81.8 %
Tot. Days	22		22	

Table 13: Number of times (days) a model is better than the other in terms of Bayesian Information Criterion (BIC). The results are also reported in percentage.

### B.4 Integrated vs stationary score-driven specifications

In this appendix, we take into consideration different DCS specifications of the AMH model with the aim to assess whether a stationary (autoregressive) or integrated score-driven model describes the data better. We compare the two different score-driven models using the BIC and the Out-of-Sample Likelihood (OSL). The latter quantity is defined as the logarithmic likelihood evaluated with the data for day  $\tau$  and with the parameters estimated for day  $\tau - 1$  ( $\theta^{(\tau-1)}$ ) and calculated as

$$\text{OSL} := \mathcal{L}(y^{(\tau)} \mid b_{0,t}^{(\tau-1)}, \mathcal{F}^{(\tau-1)}, \theta^{(\tau-1)}), \quad (24)$$

where  $y^{(\tau)}$  is the vector of variables,  $b_{0,t}^{(\tau)}$  is the time-varying parameter,  $\mathcal{F}^{(\tau)}$  is the available information set and  $\theta^{(\tau)}$  is the vector of static parameter of day  $\tau$ , with  $\tau = 1, \dots, 22$ . The DCS versions proposed for the AMH model are the following

$$\text{SD-AR} \quad b_{0,t+1} = \omega + \beta b_{0,t} + \alpha x_t (r_t - \mu_t^{(1)}), \quad (25)$$

$$\text{SD-INT} \quad b_{0,t+1} = b_{0,t} + \alpha x_t (r_t - \mu_t^{(1)}), \quad (26)$$

Section 2 of the main paper introduces and discusses Eqs. (25) and (26). The two specifications characterize the DCS stationary or integrated dynamics of the time-varying impact parameter in the AMH model of Eqs. (7) and (11). Tables 14 and 15 show that the integrated specification (SD-INT) performs better than the stationary one in terms of both in-

and out-of-sample criteria.

	MSFT		AMZN	
SD-AR	0	0.00 %	0	0.00 %
SD-INT	22	100 %	22	100 %
Tot. Days	22		22	

Table 14: Number of days out of 22 a DCS specification model performs better than the other one according to the BIC. Results are also reported in percentage.

	MSFT		AMZN	
SD-AR	4	19.9 %	6	28.6 %
SD-INT	17	80.1 %	15	71.4 %
Tot. Days	21		21	

Table 15: Number of days out of 22 a DCS specification model performs better than the other one according to the OLS. Results are also reported in percentage.

## Appendix C Estimation and Initialization details

### C.1 Estimation

Given the vector of unknown parameters  $\theta \in \Theta \subset \mathbb{R}^D$ , we maximize the log-likelihood function of Eq. (6) to find maximum likelihood estimates (MLE)  $\hat{\theta}$ , as in Eq. (13). The steps are the following:

1. Estimate the parameters of the AH model using OLS and get  $\hat{\theta}^{AH}$ . We split  $\hat{\theta}^{AH}$  in two components: a) the parameters of the  $r_t$  equation  $\hat{\theta}_r^{AH}$  and b) the parameters of the  $x_t$  equation  $\hat{\theta}_x^{AH}$ . Thus, we have  $\hat{\theta}^{AH} = (\hat{\theta}_r^{AH}, \hat{\theta}_x^{AH})$ .
2. Estimate the parameters of the AMH model by initializing the likelihood function with a parameter vector  $\hat{\theta}_0^{AMH} = (\hat{\theta}_r^{AH}, 2 \cdot \hat{\theta}_x^{AH})$ . The return equations of the AH and AMH model are the same. For this reason, we initialize  $\hat{\theta}_r^{AMH}$  with  $\hat{\theta}_r^{AH}$ . Concerning the trade sign equation, we approximate  $x_t$  with  $2\pi_t - 1 = \tanh(\mu_t^{(2)}/2)$ . When  $\mu_t^{(2)} \simeq 0.0$ ,

by linearization we obtain that  $2\pi_t - 1 \simeq \mu_t^{(2)}/2$  and then  $x_t \simeq \mu_t^{(2)}/2$ . Under this regime, we guess the following linear relation between the AH and AMH trade sign parameters:  $\hat{\theta}_x^{AH} \simeq \hat{\theta}_x^{AMH}/2$ , hence the initialization rule.

3. Maximize the log-likelihood of the SDAMH model initializing the constant parameters with the ones estimated for the AMH model. At this stage, the initial value of the time-varying parameters  $b_{0,t}$  and  $\sigma_t$  enter the procedure. We initialize them with the constant instantaneous impact  $b_0$  and volatility  $\sigma_1$  estimated for the AMH model.

The maximization of the log-likelihood is carried out using a standard quasi-Newton optimization method.

## **Appendix D    The role of the market state on the information content of a trade**

In this appendix, we explore in more detail the role of the market state in determining the LRCIRF and thus the information content of a trade. We do this in two ways: first, we restrict the regression analysis of Section 3.4 to an intraday period when the integrated dynamics of the instantaneous impact parameter  $b_{0,t}$  is less evident. In the second approach, we perform the regression of LRCIRF on the market state by considering a non-linear constant parameter model, namely the AMH model. The first analysis can also be seen as a robustness check of the results of Section 3.4. We restricted the regression analysis to the period from 10:30 onward and, in doing so, we removed from the analysis the period when the highest values of  $b_{0,t}$  are observed (see Figure 1) restricting the effects of the integrated dynamics of the time-varying parameter on the regression. The results, reported in Table 16, indicate that the sign of the relevant coefficients is statistically significant and consistent with the unconditional results of Table 3. In fact, it is  $\gamma_1 > 0$ ,  $\gamma_2 < 0$  and  $\gamma_3 > 0$ . The  $R^2$  remains high in all cases, ranging from 0.356 to 0.443. Thus, the role of the state is significant also when

the instantaneous impact is relatively small. However, we notice some differences. For the regression of Eq. (17) the value of  $\gamma_1$  is on average small when compared with the previous estimates but still statistically significant. Despite the reduction in the variability range of  $b_{0,t}$ , the effect of the state on the cumulative long-term impulse response function ( $\gamma_2$ ) is roughly the same and still significant. On the other hand, the coefficients  $\gamma_3$  of the regression of Eq. (18) are lower (in absolute value) than those estimated in Section 3.4.

### Regression results - I

	MSFT				AMZN			
	$\gamma_0$	$\gamma_1$	$\gamma_2$	$\gamma_3$	$\gamma_0$	$\gamma_1$	$\gamma_2$	$\gamma_3$
Est	$8.516 \cdot 10^{-6}$	0.901	$-1.151 \cdot 10^{-1}$	-	$7.701 \cdot 10^{-6}$	1.277	$-8.420 \cdot 10^{-2}$	-
$\#\{p > 5\%\}$	3	3	2	-	3	3	3	-
$R^2$	0.443				0.403			
Est	$8.254 \cdot 10^{-6}$	-	-	$-4.637 \cdot 10^{-2}$	$2.794 \cdot 10^{-5}$	-	-	$-5.520 \cdot 10^{-2}$
$\#\{p > 5\%\}$	4	-	-	4	4	-	-	3
$R^2$	0.356				0.394			

Table 16: Results of regressions of models of Eqs. (17) (top) and (18) (bottom). Temporal average of the point estimates (Est), of the number of times we do not reject the null hypothesis at 5% level  $\#\{p > 5\%\}$ , and the  $R^2$  in case of "low" range of  $b_{0,t}$ .

To deepen our understanding of the role of the state on the information content of trade (and thus LRCIRF), we performed a regression analysis for the AMH model, for which the instantaneous impact parameter  $b_0$  is constant. Being a non-linear model, the IRF depends on the history of the process and the regression we perform, namely

$$\text{LRCIRF}_t = \gamma_0 + \gamma_2 |\mu_{t-1}^{(*)}| + \eta_t. \quad (27)$$

aims at measuring the strength and significance of their relationship. Table 17 shows that  $\gamma_2$  is negative and significant for both stocks, indicating a role for the state in the long-term cumulative response function also when the model neglects the impact of time variations. Finally, the small number of times the null hypothesis of no dependence is rejected and high  $R^2$  strengthens the evidence that the state has a relevant role in determining the information

content of stock trades.

Regression results - II									
	MSFT					AMZN			
	$\gamma_0$	$\gamma_1$	$\gamma_2$	$\gamma_3$	$\gamma_0$	$\gamma_1$	$\gamma_2$	$\gamma_3$	
Est	$1.369 \cdot 10^{-5}$	-	$-4.781 \cdot 10^{-2}$	-	$2.479 \cdot 10^{-5}$	-	$-3.214 \cdot 10^{-1}$	-	
$\#\{p > 5\%\}$	3	-	3	-	4	-	3	-	
$R^2$	0.372				0.339				

Table 17: Results of regressions of Eq. (18) for the AMH model. Temporal average of the point estimates (Est), of the number of times we do not reject the null hypothesis at 5% level  $\#\{p > 5\%\}$ , and the  $R^2$ .

## Appendix E Derivation and numerical validation of the permanent impact coefficient

### E.1 Derivation of the coefficient

We start considering the SDAMH model given by Eqs. (9), (10), and (11). To shorten the notation, we define  $\bar{r}_t := \sum_{j=t-M}^{t-1} r_j/M$  and  $\bar{x}_t := \sum_{j=t-M}^{t-1} x_j/M$ . Replacing Eq. (9) in Eq. in (20), we obtain

$$\hat{\beta}_t^{(s)} := \frac{\bar{r}_t}{\bar{x}_t} = a_1 \frac{\bar{r}_{t-1}}{\bar{x}_t} + \frac{1}{M} \frac{\sum_{j=t-M}^{t-1} b_{0,j} x_j}{\bar{x}_t} + b_1 \frac{\bar{x}_{t-1}}{\bar{x}_t} + \bar{b}_{10} \frac{\frac{1}{L_1-1} \sum_{i=2}^{L_1} \bar{x}_{t-i}}{\bar{x}_t} + \bar{b}_{100} \frac{\frac{1}{L_2-L_1-1} \sum_{i=L_1+1}^{L_2} \bar{x}_{t-i}}{\bar{x}_t}. \quad (28)$$

Relying on the fact that the return process  $r_t$  typically shows weak evidence of serial correlation, from now on we assume that the local average of  $r_t$  over intervals of  $M$  observations does not depend on time, i.e.,  $\bar{r}_{t-i} = \bar{r}$  for any  $i \geq 0$ . It readily follows that the r.h.s. in the first line in Eq. (28) boils down to

$$a_1 \frac{\bar{r}}{\bar{x}_t} = a_1 \hat{\beta}_t^{(s)}.$$

Consistent with the long-memory property of the order flow, the local average of the process  $x_t$  assumes different values when computed at different intervals intraday. We rename the first term in the second line of Eq. (28) and approximate it as follows

$$\bar{b}_{0,t}^{(s)} := \frac{\frac{1}{M} \sum_{j=t-M}^{t-1} b_{0,j} x_j}{\bar{x}_t} \simeq \frac{\frac{1}{M} \bar{b}_{0,t} \sum_{j=t-M}^{t-1} x_j}{\bar{x}_t} = \bar{b}_{0,t}, \quad (29)$$

where  $\bar{b}_{0,t}$  is the time-average of  $b_{0,j}$ ;  $\bar{b}_{0,t}^{(s)}$  is the order-flow-weighted average of  $b_{0,j}$ . Both averages are computed over the interval from  $t - M$  to  $t - 1$ <sup>20</sup>. Eventually, after defining

$$\omega_t^{(1)} := \frac{\bar{x}_{t-1}}{\bar{x}_t}, \quad \omega_t^{(L_1)} := \frac{1}{L_1 - 1} \frac{\sum_{i=2}^{L_1} \bar{x}_{t-i}}{\bar{x}_t}, \quad \omega_t^{(L_2)} := \frac{1}{L_2 - L_1} \frac{\sum_{i=L_1+1}^{L_2} \bar{x}_{t-i}}{\bar{x}_t},$$

Eq. (28) reduces to

$$\hat{\beta}_t^{(s)} \simeq a_1 \hat{\beta}_t^{(s)} + \bar{b}_{0,t} + b_1 \omega_t^{(1)} + \bar{b}_{10} \omega_t^{(L_1)} + \bar{b}_{100} \omega_t^{(L_2)}, \quad (30)$$

from which we get the permanent price impact function for the SDAMH model as

$$\hat{\beta}_t^{(s)} \simeq \frac{\bar{b}_{0,t} + b_1 \omega_t^{(1)} + \bar{b}_{10} \omega_t^{(L_1)} + \bar{b}_{100} \omega_t^{(L_2)}}{1 - a_1}. \quad (31)$$

Notice that, coherently with the nonlinearity of the SDAMH model and the presence of a time-varying parameter, the permanent impact coefficient of Eq. (31) depends on time both through the market state ( $\omega_t^{(1)}$ ,  $\omega_t^{(L_1)}$  and  $\omega_t^{(L_2)}$ ) and through the dynamic instantaneous impact coefficient ( $\bar{b}_{0,t}$ ). It is important to recall that the daily estimates of  $b_0$  for the AMH model are similar to the unconditional daily average of  $b_{0,t}$ . For this, the permanent impact function of the AMH model can be deduced from its score-driven version, replacing the average of the estimated  $\bar{b}_{0,t}$  in the intraday intervals of  $M$  observations with  $b_0$  in Eq. (31).

---

<sup>20</sup>Applying the law of iterated expectations and assuming that  $b_{0,t}$  is independent from  $x_t$ , it is easy to show that  $\bar{b}_{0,t}^{(s)} = \bar{b}_{0,t}$ . In the case of real data where  $b_{0,t}$  depends on  $x_t$ , the two quantities are similar. In our sample, the mean absolute deviation is  $3.262 \cdot 10^{-5}$  for MSFT and  $1.370 \cdot 10^{-5}$  for AMZN, and the maximum absolute deviation is  $1.973 \cdot 10^{-4}$  for MSFT and  $1.444 \cdot 10^{-4}$  for AMZN.



We finally get the permanent impact function of the AMH model as

$$\hat{\beta}_t^{(s)} \simeq \frac{b_0 + b_1\omega_t^{(1)} + \bar{b}_{10}\omega_t^{(L_1)} + \bar{b}_{100}\omega_t^{(L_2)}}{1 - a_1}. \quad (32)$$

It is easy to show (following the same procedure) that for a linear SVAR( $p$ ) model, the estimated coefficient is given by

$$\hat{\beta}^{(s)} = \frac{\sum_{i=0}^p b_i}{1 - \sum_{i=1}^p a_i}. \quad (33)$$

## E.2 Monte Carlo simulated permanent impact function

In this appendix, we use Monte Carlo simulations to assess whether the SDAMH approach provides estimates of the permanent impact which are coherent with the ones obtained using the standard regression approach. The permanent impact is often estimated (see, for example, Cartea and Jaimungal (2016)) by performing the linear regression of price changes over a given time interval versus the contemporaneous aggregated order flow, that is, the difference between the volume of buy and sell market orders. Since our model considers price returns and trade signs, we compare the SDAMH estimation with the one obtained from the linear regression of aggregated return versus the contemporaneous net order flow sign, i.e. the difference between the number of buy and sell trades. Moreover, we will consider aggregation in trade time rather than in physical time, since Hasbrouck's model and all the modifications we propose are defined in trade time. For the Monte Carlo experiment, we simulate the  $r_t$  and  $x_t$  SDAMH models of Eqs. (9), (10) and (11) using parameters similar to the estimates obtained on real data <sup>21</sup> and then we compute the permanent impact coefficient on the simulations  $S$  using the two approaches. For the SDAMH model, we estimate the static parameters on a simulated series of observations  $T = 10,000$ , maximizing the log-likelihood function of the model. Then, we obtain the filtered estimates of the time-varying parameter  $b_{0,t}$ . Consid-

---

<sup>21</sup>The parameters are the monthly estimates of MSFT (see Table (2)).

ering aggregation windows of  $M = 101$  observations <sup>22</sup>, we compute the permanent impact coefficients  $\hat{\beta}_t^{(s)}$  of Eq. (21) to get a series of  $T/M$  permanent impacts. Then, we compute the average of  $\hat{\beta}_t^{(s)}$ 's over the  $T/M$  intervals. We repeat the experiment  $S = 1,000$  times. In the end, we get the average permanent impact coefficient of the SDAMH computed on the  $S$  replications, named  $\beta^{(SD)}$ . Although SDAMH provides time-varying estimates of permanent impact by nature, averaging over the  $T/M$  intervals in each simulation allows us to derive an average value of the permanent impact coefficient of the SDAMH model, which can be compared to the static estimate of the regression model. For the regression approach, we consider the simulated series with  $T = 10,000$ , we aggregate data on intervals  $M = 101$ , and we use regression of the price return in each interval versus the contemporaneous difference between buy and sell trades to estimate the permanent impact coefficient. Finally, we name  $\beta^{(reg)}$  the permanent impact coefficient of the regression computed as the average on the  $S = 1,000$  simulations. Table 18 shows the estimates of the permanent impact and some summary statistics on Monte Carlo simulations of the two approaches. From the table, we note that the two estimates show similar mean and median (Med) values. Moreover, the two coefficients are properly identified: they exhibit low standard deviation and quantile range values. However, the standard deviation and the quantile range of the  $\beta^{(SD)}$  are lower than the ones of the  $\beta^{(reg)}$  indicating that the SDAMH provides more accurate estimates than the ones the regression approach on aggregated data.

---

<sup>22</sup>Since the  $x_t \in \{-1, +1\}$ , we use  $M$  odd to avoid issues in the estimation of  $\hat{\beta}_t^{(s)}$  when aggregating data.

**Monte Carlo results for the permanent impact function**

	Mean	Med	Std	$\Delta q$
$\beta^{(SD)}$	$7.511 \cdot 10^{-6}$	$7.508 \cdot 10^{-6}$	$6.500 \cdot 10^{-7}$	$2.250 \cdot 10^{-7}$
$\beta^{(reg)}$	$7.406 \cdot 10^{-6}$	$7.423 \cdot 10^{-6}$	$1.352 \cdot 10^{-6}$	$3.010 \cdot 10^{-7}$

Table 18: Summary statistics of the permanent impact for SDAMH model ( $\beta^{(SD)}$ ) and for regression model ( $\beta^{(reg)}$ ): Mean, Median (Med), standard deviation (Std), the difference between the quantile in 95% and the quantile at 5% ( $\Delta q$ ).

### Filtered time-varying parameters and LRCIRF<sub>t</sub>

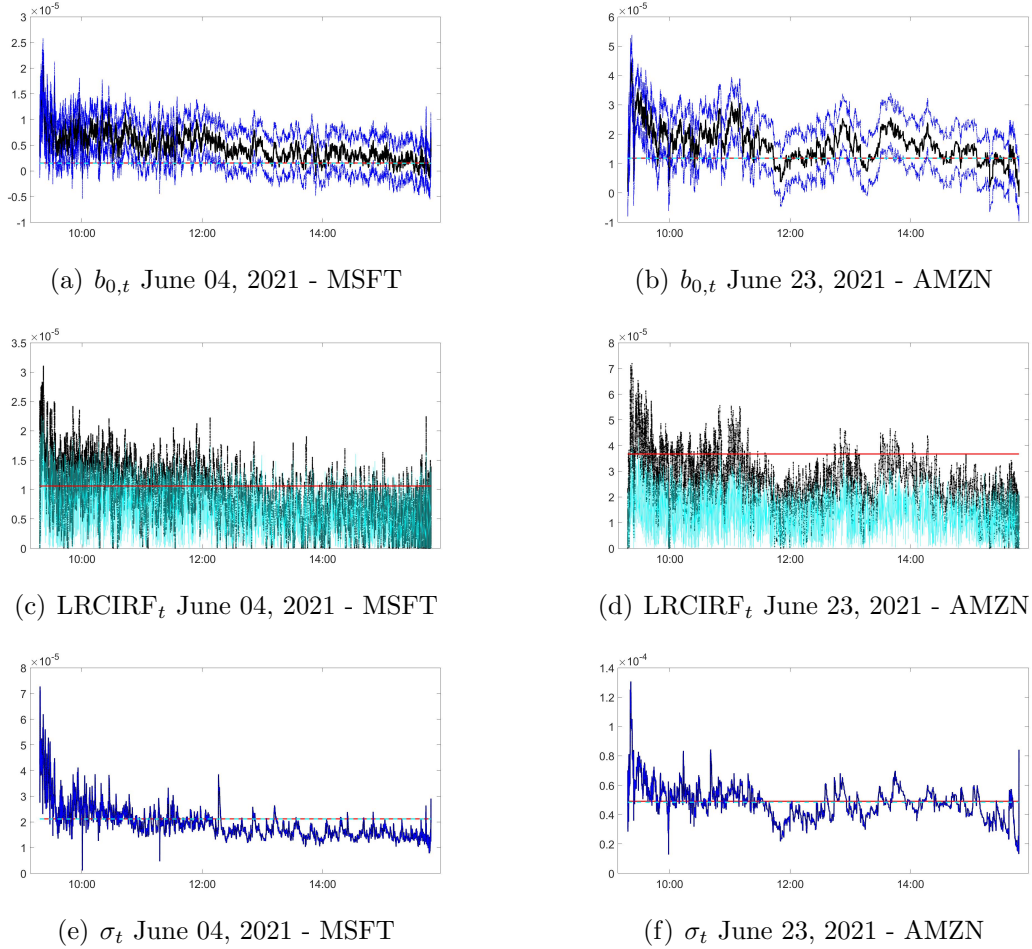


Figure 3: Top panels: Estimates of the time-varying instantaneous impact parameter of the SDAMH model (black solid lines) and 95% confidence bands (blue dashed lines). Middle panels: Estimates of the long-term cumulative impulse response function (LRCIRF<sub>t</sub>) of the SDAMH model (black dotted lines), of the AMH model (cyan dashed lines), and of the AH model (red solid lines). Bottom panels: Estimates of the time-varying volatility of the SDAMH model (black solid lines) and 95% confidence bands (blue dashed lines). Results for MSFT on June 04, 2021 and AMZN on June 23, 2021.

### Estimates of $\text{LRCIRF}_t$ , $b_{0,t}$ and $|\mu_{t-1}^*|$ during an FOMC day

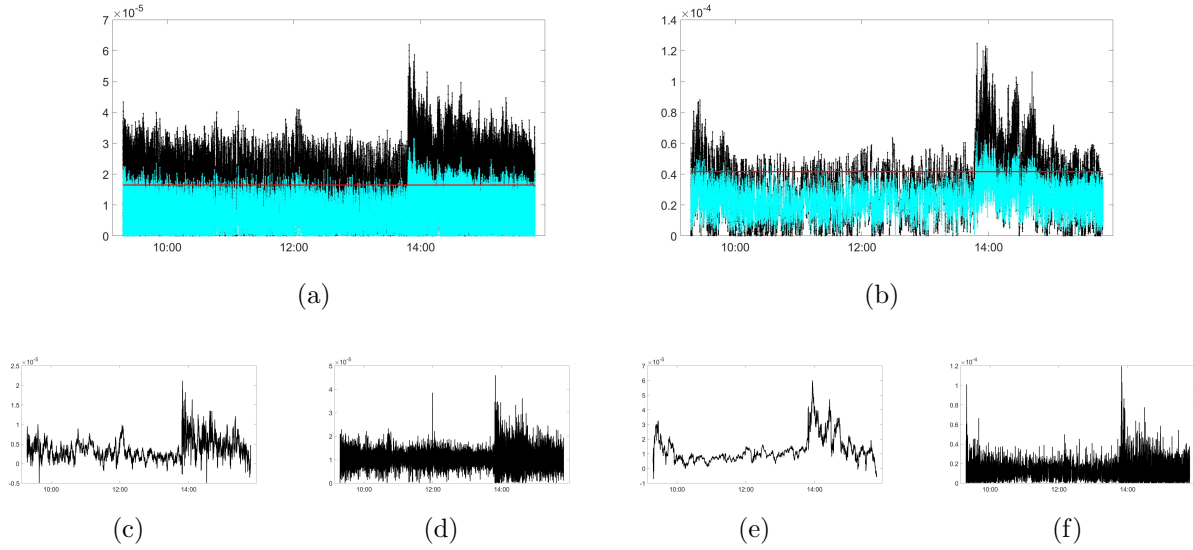


Figure 4: Panel (a) and (b): long-run cumulative impulse response ( $\text{LRCIRF}_t$ , y-axis) for the SDAMH model (black dotted lines), for the AMH model (cyan dashed lines), and for the AH model (red solid lines). Time in hours and minutes (hh:mm, x-axis). Panel (c) and (d): instantaneous impact  $b_{0,t}$ . Panel (e) and (f): absolute state  $|\mu_{t-1}^*|$ . Results for MSFT (left panels) and AMZN (right panels) on June 16, 2021.

### $\text{CIRF}_{t,h}$ estimates during FOMC - I

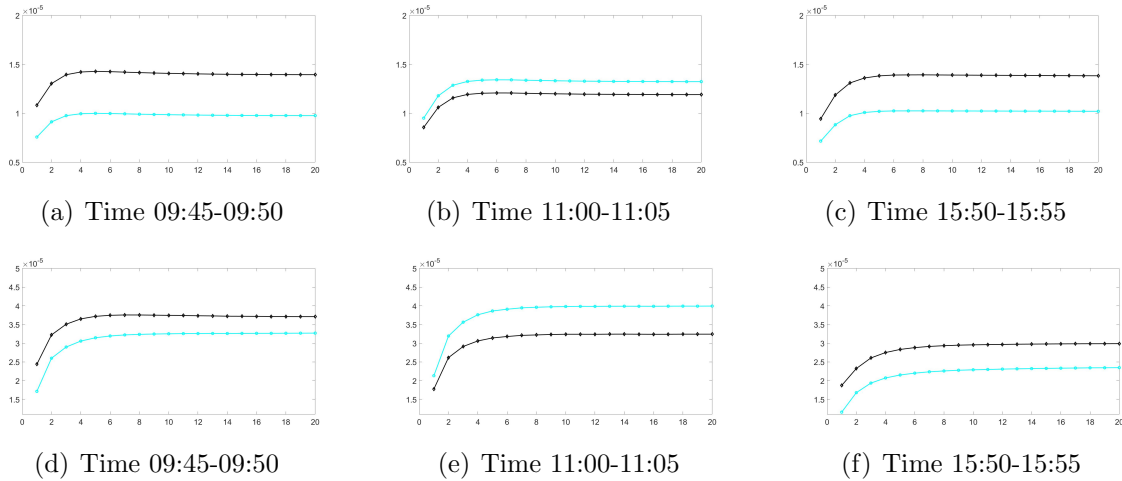


Figure 5: Cumulative response  $\text{CIRF}_h$  for  $h = 1, \dots, H$  of SDAMH (black diamonded lines), and for AMH (cyan circled lines) model. The lines are average over trades in the specified intervals corresponding to different market phases, namely the opening (left), calm period (middle), and closing (right). Results for MSFT (top) and AMZN (bottom) on June 16, 2021.

## CIRF<sub>t,h</sub> estimates during FOMC - II

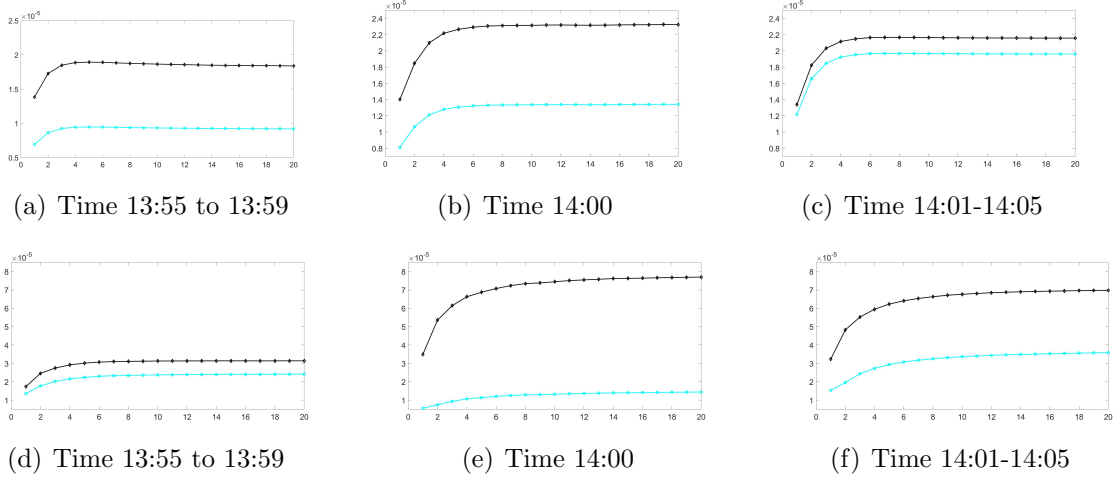


Figure 6: Cumulative response CIRF<sub>h</sub> for  $h = 1, \dots, H$  of SDAMH (black diamonded lines), and for AMH (cyan circled lines) model. The lines are averages over trades in the specified intervals corresponding to different periods around the FOMC announcement, namely before (left), during (middle), and after (after) the event. Results for MSFT (top) and AMZN (bottom) on June 16, 2021.

## Time-varying estimates of permanent impact

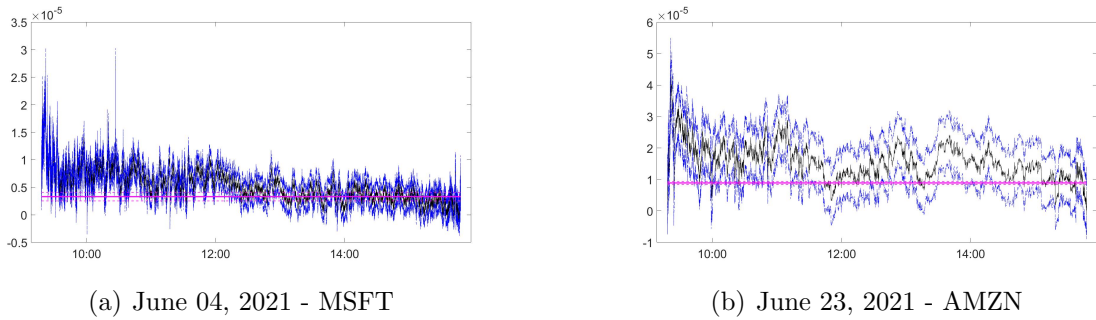
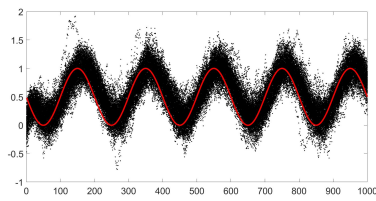
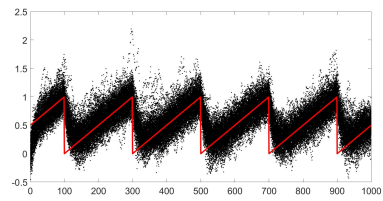


Figure 7: Estimates of  $\hat{\beta}_t^{(s)}$  (black lines) and time-varying 95% confidence bands (blue dashed lines), with a window of  $M = 101$ . Estimated regression  $\hat{\beta}_1^{(reg)}$  (dash-dotted magenta lines) with 1 minute aggregated data and bands (dashed magenta lines). Results for MSFT on June 04, 2021 (a) and AMZN on June 23, 2021 (b).

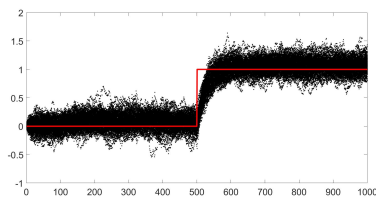
### Filtering misspecified dynamics on MCs



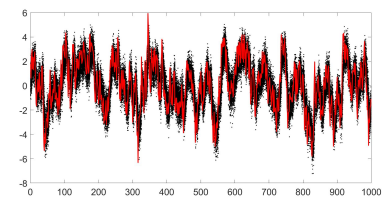
(a) Fast Sine



(b) Ramp



(c) Step



(d) AR(1)

Figure 8: Temporal evolution of  $b_{0,t}^*$  for the considered DGPs (red solid lines) and filtered dynamics from the SDAMH (black dots).